HIGH-VOLUME SAMPLING SYSTEM TO MEASURE METHANE EMISSIONS FROM NATURAL GAS REFUELING INFRASTRUCTURE

by

Hadyan Sani Ramadhan

B.S., University of Florida, 2015

A THESIS SUBMITTED IN PARTIAL FULFILLMENT OF

THE REQUIREMENTS FOR THE DEGREE OF

MASTER OF APPLIED SCIENCE

in

THE FACULTY OF GRADUATE AND POSTDOCTORAL STUDIES

(Mechanical Engineering)

THE UNIVERSITY OF BRITISH COLUMBIA

(Vancouver)

April 2020

The following individuals certify that they have read, and recommend to the Faculty of Graduate and Postdoctoral Studies for acceptance, a thesis entitled:

High-Volume Sampling System to Measure Methane Emissions from Natural Gas Refueling Infrastructure

submitted by Hadyan Sani Ramadhan in partial fulfillment of the requirements for

the degree of Master of Applied Science

in Mechanical Engineering

Examining Committee:

Walter Mérida, Professor, Mechanical Engineering, UBC
Supervisor

Patrick Kirchen, Associate Professor, Mechanical Engineering, UBC
Supervisory Committee Member

Naomi Zimmerman, Assistant Professor, Mechanical Engineering, UBC
Supervisory Committee Member

Abstract

Natural gas has gained attraction as an alternative fuel for heavy-duty vehicles due to its lower prices and carbon dioxide (CO_2) emissions as compared to diesel. However, methane is the main component of natural gas, and it is a potent greenhouse gas (GHG). The global warming potentials (GWPs) of methane are 86 and 34 times as high as those of CO_2 in 20- and 100-year horizons, respectively. The potential of natural gas to reduce GHG emissions from heavy-duty vehicles can be undermined if enough methane is emitted along the natural gas supply chain.

A high-volume sampling (HVS) system was developed to accurately quantify methane emissions from the pump-to-tank (PTT) segment or the natural gas refueling infrastructure. This segment is the least documented portion in the life cycle analysis of natural gas. The accuracy of the HVS system was validated by comparing the measurements with known flow rates of injected methane and CO_2. The results showed that the HVS system was capable of measuring steady-state leaks and transient emissions with a maximum uncertainty of 6.6%.

The utility of the HVS system was demonstrated to measure methane emissions from a pilot and fully-operational time-fill compressed natural gas (CNG) refueling station. A data set of component-level emission rates from compressors, component and nozzle leaks, and nozzle venting events was generated. The results showed that compressors were a significant source of emissions in the pilot station, contributing 88.6% to the annual emissions. Prior to regularly scheduled maintenance, compressor emissions and nozzle leaks in the fully-operational station contributed 32.9% and 66.6% to the annual emissions, respectively. The PTT methane emissions from the pilot and fully-operational stations were 1.4 ± 0.8% and 0.7 ± 0.7% of the total throughputs, respectively. Using these data, practical solutions were recommended and

implemented to reduce the PTT methane emissions by 80 ± 20% and 98 ± 2% in the pilot and fully-operational stations, respectively. The HVS methodology presented in this study can be applied to accurately quantify methane emissions from a wide range of natural gas refueling infrastructure including fast-fill CNG and liquefied natural gas (LNG) refueling stations, and LNG bunkering facilities.

Lay Summary

Natural gas has the lowest carbon content among fossil fuels. If used to substitute diesel as a heavy-duty transportation fuel, natural gas can reduce carbon dioxide emissions at the engine tailpipes. However, the main component of natural gas is methane, a greenhouse gas 34 times more potent than carbon dioxide. If enough methane is released to the atmosphere upstream of the end use, the life cycle greenhouse gas emissions of natural gas fuel can be similar or even greater than those of diesel. A portable measurement system was developed to quantify the amount of methane emitted from natural gas refueling stations. The system was deployed at two compressed natural gas refueling stations to measure methane emission rates from sources within the stations. The annual methane emissions from the stations were compared with the total natural gas supplied to the stations.

Preface

The original conception of this thesis work to investigate novel and practical solutions to eliminate fugitive emissions from natural gas refueling infrastructure was developed by Dr. Amir Sharafian and my supervisor, Dr. Walter Mérida. However, the direction I took with regards to formulating specific objectives and selecting the appropriate approach was largely my own undertaking.

The background review presented in Chapter 2 was completed by me with guidance from Drs. Amir Sharafian and Walter Mérida. The design, fabrication, development, and validation of the high-volume sampling system described in Chapter 3 were conducted by me with inputs from Dr. Amir Sharafian and under the supervision of Dr. Walter Mérida.

Emission measurement campaigns at two time-fill compressed natural gas refueling stations reported in Chapter 4 were conducted by Dr. Amir Sharafian and me. I completed the data post-processing and analysis, compiled reports, and presented the results to the industry partners that operate the facilities.

A version of Chapter 3 was presented by me and published as the following conference proceeding:

- **H. Ramadhan**, A. Sharafian, W. Mérida, Fugitive Methane Emissions: Development of a Mobile High-Volume Sampling System, in: ASME 2019 Int. Mech. Eng. Congr. Expo., Salt Lake City, Utah, USA, 2019. doi:10.1115/IMECE2019-11891.

I wrote most of the manuscript with inputs from Drs. Amir Sharafian and Walter Mérida.

Table of Contents

List of Tables

List of Figures

List of Abbreviations

BC	British Columbia
BHFS	Bacharach Hi Flow Sampler
CH_4	Methane
CNG	Compressed natural gas
CO_2	Carbon dioxide
DGE	Diesel gallon equivalent
EDF	Environmental Defense Fund
EIA	Energy Information Administration
GHG	Greenhouse gas
GREET	Greenhouse Gases, Regulated Emissions, and Energy Use in Transportation
GWP	Global warming potential
HVS	High-volume sampling
ICOS	Integrated cavity output spectroscopy
LCA	Life cycle assessment
LNG	Liquefied natural gas
MAF	Mass air flow
MFC	Mass flow controller
NGV	Natural gas vehicle
NO_x	Nitrogen oxides
NRCan	Natural Resources Canada
OVA	Organic vapor analyzer
PM	Particulate matter
PTT	Pump-to-tank
PTW	Pump-to-wheel
TTW	Tank-to-wheel
TVA	Toxic vapor analyzer
US	United States
WTP	Well-to-pump
WTW	Well-to-wheel

Acknowledgements

The completion of this master's thesis would not have been possible without the help of the countless people I have met in various stages of my personal, academic, and professional life.

I would like to first express my gratitude to my research supervisor, Dr. Walter Mérida, for presenting me with the opportunity to delve into working for solutions to the greatest challenge of our time. I could not have imagined a better research environment than a cross-functional team that encouraged collaboration between disciplines, academia, and the public and private sectors.

I am particularly indebted to Dr. Amir Sharafian for his mentorship. I appreciate the time and effort he has invested in providing me with ongoing guidance and feedback over the past two years. I would like to thank my research supervisory and examination committee members, Drs. Patrick Kirchen and Naomi Zimmerman, for their invaluable suggestions and stimulating insights.

My immense thanks go out to all members of Mérida Labs. In particular, I would like to thank Ezgi Kisa, Zhihao Wang, Miguel Ángel León-Luna, and Thanh Tung Nguyen for helping me navigate life as a graduate student and researcher. My appreciation also extends to my colleagues at Clean Energy Research Centre and the Engine Research Laboratory for the fruitful discussions on putting experimental methods in thermofluids into practice.

Technical and financial support from the industry partners of UBC's Natural Gas Futures is gratefully acknowledged. The cooperation of the refueling station operators in giving access to the facilities is greatly appreciated. I would also like to acknowledge the financial sponsorship provided by the Natural Sciences and Engineering Research Council of Canada (NSERC) in completing this work.

Finally, I would like to thank my precious family in Indonesia, Rosanna Wisden, and the friends I have treasured over the years for listening, encouraging, and renewing my self-belief when it faltered. Their unlimited love and support were the greatest source of motivation that kept me going through what has been an exciting yet arduous two years of graduate studies.

To my mother and father.

Chapter 1: Introduction

The 2015 Paris climate accord marked the start of collective efforts by governments around the world to combat climate change and reduce greenhouse gas (GHG) emissions. The agreement set a limit of 1.5°C for the global temperature rise by the end of this century as compared to pre-industrial levels by reducing the amount of GHGs emitted into the atmosphere [1]. Substituting petrochemical fuels, such as diesel and gasoline, with natural gas has been considered as a bridge solution to reduce carbon dioxide (CO_2) emissions from the transportation sector [2]. Reducing GHG emissions in the near-term would ensure that more options would be available toward the end of the century to meet the overarching objective of the Paris Agreement.

This chapter describes the background and motivation that drive the inception and the work encompassed in this thesis. The role of natural gas as a transportation fuel for heavy-duty vehicles and the importance of considering methane (CH_4) emissions from the natural gas fuel supply chain are discussed. Finally, the objectives and structure of the thesis are presented.

1.1 Natural Gas as a Transportation Fuel for Heavy-Duty Vehicles

Natural Resources Canada (NRCan) estimated that the transportation sector consumed 2,683 PJ or 21% of Canada's primary energy supply in 2016 [3]. Gasoline and diesel accounted for 58% and 28% of the total fuel mix, respectively, while natural gas accounted for less than 1% [3]. From 2000 to 2017, GHG emissions from the transportation sector increased by 19% from 146 to 174 Mt CO_2e [4]. Within the same timeframe, the GHG emissions from the heavy-duty transportation sector grew by 53% from 43 to 66 Mt CO_2e [4]. Several factors, including increased inter-provincial and international trades, and online commerce [3], contributed to this GHG

emission growth rate, which is almost 2.8 times greater than that of the whole transportation sector between 2000 and 2017. The heavy-duty transportation sector traditionally uses diesel fuel as its primary energy source [5].

In the long term, decarbonization of the global transportation system would be required if the 1.5°C goal of the Paris climate accord were to be achieved. In a 100% renewable future, it is expected that light-duty transportation would be mainly powered by batteries and grid electricity. On-road heavy-duty vehicles would be powered by hydrogen fuel cells and renewable methane-fueled internal combustion engines [6].

In the near- to medium-term, natural gas has been regarded as a means of cutting transportation-related GHG emissions [2]. Compared to diesel, natural gas can theoretically reduce tailpipe CO_2 emissions by approximately 25%. Although there is a wide range of estimates in the literature, the actual reductions in CO_2 emissions are generally not as high due to the lower efficiency of the current-technology natural gas engines. Nevertheless, advancement in natural gas engine technology, as well as improvements in other factors affecting the fuel economy such as vehicle aerodynamics, weight, and tire rolling resistance, are expected to narrow the gap between actual and theoretical reductions in CO_2 emissions [7].

Natural gas also provides environmental benefits in terms of air pollutants. Natural gas vehicles (NGVs) emit lower nitrogen oxides (NO_x) than their diesel counterparts. Several studies showed that natural gas freight trucks consistently emit 42% to 95% lower NO_x as compared to diesel freight trucks [8–10]. The tailpipe particulate matter (PM) emissions of NGVs are similar to those of diesel trucks [8]. However, NGVs' compliance with the PM emission standards is achieved without the need of particulate filter in the exhaust aftertreatment system. This is due to the soot-free combustion of natural gas [5].

From an economic perspective, natural gas is considered one of the most attractive alternative fuels to power the heavy-duty transportation sector [8,11]. Resulting from the shale gas revolution, the United States (US) Energy Information Administration (EIA) projected that the prices of natural gas would remain lower than those of oil for the next 30 years [12]. Canada's position as the fourth largest producer of natural gas in the world, as well as the integration of Canada's natural gas markets with those of the US, result in the abundant supply of low-cost natural gas in North America [13].

The adoption of natural gas as an on-road transportation fuel poses minimal risks as natural gas engine and fuel dispensing technologies are mature and readily available [2,14]. Natural gas, in the form of compressed natural gas (CNG), has been widely used as an on-road transportation fuel for light-duty, transit, and refuse applications [15]. Liquefied natural gas (LNG) is a more energy-dense fuel and currently being developed as a diesel substitute for long-distance road transportation [2].

Based on the potential market penetration and growth of natural gas, researchers from the University of California, Davis developed scenarios for natural gas fuel adoption in California by 2035. CNG would be used in medium-duty delivery and short-haul heavy-duty trucks. They estimated that the number of CNG vehicles would grow from 48,000 in 2015 to 66,000 in 2035. LNG would fuel 14% of the 70,000 long-haul heavy-duty freight trucks, and the number of public LNG refueling stations would increase from 46 in 2017 to 100 in 2035 to serve long-haul freight trucks operating along the key freight corridors [15]. Several scenarios also suggested even more optimistic projections with natural gas vehicles representing half of heavy-duty fleet in the US by 2035 [16].

1.2 Well-to-Wheel Greenhouse Gas Emissions of Natural Gas Fuel

Despite the cost advantage and already demonstrated technologies, the widespread adoption of natural gas as a transportation fuel has been hampered by its uncertain environmental performance [2,15]. The initial public perception is that switching from diesel to natural gas fuel is climatically beneficial as the combustion of natural gas produces less CO_2 per unit usable energy. However, recent research studies revealed that methane emissions across the natural gas fuel supply chain could erode the GHG benefits that are gained at the tailpipe [17]. Methane, the main component of natural gas, is a potent GHG with global warming potentials (GWPs) 86 and 34 times as high as those of CO_2 in 20- and 100-year horizons, respectively. Atmospheric methane dissociates into other components after its estimated lifetime of 11 years, leading to decrease in its radiative forcing [18]. While the GWP of methane decreases over time, its short-term impact could be significant. Therefore, the amount of uncontrolled methane release across the natural gas supply chain should be considered when assessing the effectiveness of using CNG and LNG fuels in cutting transportation-related GHG emissions.

Figure 1 shows the well-to-wheel (WTW) supply chain of natural gas fuel. It comprises the well-to-pump (WTP) and pump-to-wheel (PTW) segments. The boundary of the WTP segment encompasses natural gas production, gathering and processing, transmission and storage, and natural gas fuel production and distribution. The PTW segment is composed of the pump-to-tank (PTT) segment, which includes CNG and LNG refueling stations, and the tank-to-wheel (TTW) segment or the use of natural gas fuels by vehicles [8,19].

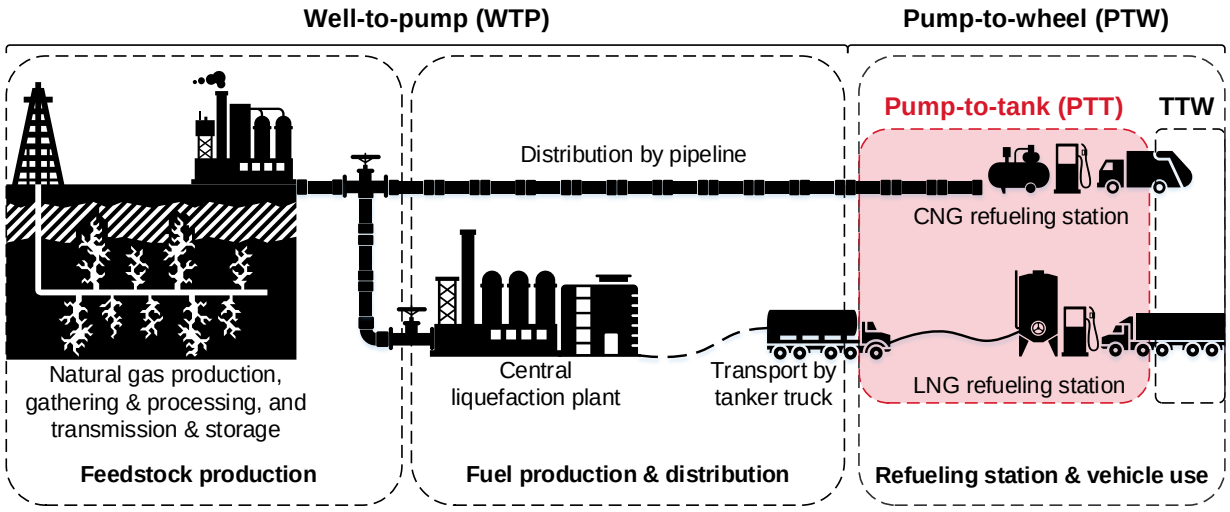

Figure 1. The well-to-pump (WTP) and pump-to-wheel (PTW) segments of the natural gas fuel supply chain. The highlighted box in red shows the pump-to-tank (PTT) system boundary considered in this thesis.

As shown in Figure 1, the natural gas fuel supply chain consists of the CNG and LNG fuel pathways. In the CNG fuel pathway, natural gas is transported to the CNG refueling station by pipeline and compressed to a pressure between 16.5 and 24.8 MPa (2400 and 3600 psi). In fast-fill CNG stations, CNG is stored in pressurized vessels before being dispensed to natural gas vehicles. In time-fill CNG stations, high-pressure natural gas is dispensed directly from the compressors into vehicle fuel tanks [15,20]. In the LNG fuel pathway, natural gas feedstock is transported using pipeline from the supply site to a central liquefaction plant. Following liquefaction, LNG is transported using tanker trucks and offloaded to storage tanks in refueling stations. LNG is then dispensed into vehicle tanks to power the engines [2,14,15].

A natural gas life cycle assessment (LCA) conducted by Tong et al. [11] concluded that CNG and LNG fuels, as compared to diesel, increased the life cycle GHG emissions of Class 8 trucks by 0% to 3% and 2% to 13%, respectively. Methane leakage across the natural gas fuel supply chain plays a key role in determining whether CNG and LNG fuels are net GHG emission reducers [11]. Another study by Camuzeaux et al. [17] claimed that no climate benefits would be

gained by switching from diesel to natural gas fuel if methane emissions in the PTW segment were high enough. Speirs et al. [7] also indicated that, although switching to natural gas could reduce WTW GHG emissions by 16% in the best-case scenario, the worst-case scenario suggested that natural gas heavy-duty vehicles emitted more WTW GHG than their diesel counterparts. In the context of natural gas fuel use in Canada and the province of British Columbia (BC), Sharafian et al. [21] conducted a LCA to evaluate the impact of replacing diesel with LNG in the heavy-duty transportation sector. They concluded that the WTW GHG emissions would change by +1.7% to +24% for Canada, and by −8% to +16% for BC under 20- and 100-year horizons, respectively, if there were no reductions in the current WTW methane emissions. They showed that if 2.4% methane (mass basis) is emitted along the LNG supply chain in Canada, using LNG as a fuel in heavy-duty trucks produces the same amount of GHG emissions as their diesel counterparts in a 100-year time horizon. From the life cycle standpoint, disagreement regarding the environmental benefits of natural gas fuel makes the development of a reliable methane emission database necessary if natural gas is to power a significant percentage of heavy-duty vehicles in the years to come [2,17].

A large number of studies, such as the methane research series supported by the Environmental Defense Fund (EDF), have been conducted to investigate the WTP methane emissions [22,23,32,33,24–31]. A significant data gap existed in the PTW segment until Clark et al. [19] investigated methane emissions from the natural gas refueling infrastructure and natural gas-fueled heavy-duty vehicles. PTW emission data included in models such as the Greenhouse Gases, Regulated Emissions, and Energy Use in Transportation (GREET) developed by Argonne National Laboratory only include TTW methane emissions from vehicle tailpipes and engine crankcases [16]. The PTT is the least well-documented portion in the entire life cycle analysis of

natural gas fuel due to the lack of environmental regulations to abate methane emissions from this segment.

In this thesis, a methane emission quantification system is designed and developed. The capability of this system to quantify methane emissions from the PTT segment of the CNG fuel supply chain is assessed. The fence line of a time-fill CNG refueling station represents the PTT system boundary considered in this thesis. Continuous leaks from station components and nozzles are characterized, and emissions from compressors, nozzle venting events, and nozzle disconnects are quantified.

1.3 Objectives and Approach

The main objective of this thesis work is to quantify PTT methane emissions from natural gas refueling infrastructure within the context of the province of British Columbia with potentials to extend the results to Canada at large. A better understanding on the magnitude of methane emissions from the PTT segment would reduce the uncertainty in assessing the climate impacts of switching from diesel to natural gas fuel. Specifically, this thesis aims to:

- Generate a data set of component-level methane emissions for sources within a time-fill CNG refueling station;
- Quantify the PTT methane emissions from time-fill CNG refueling stations for heavy-duty vehicles;
- Suggest abatement and mitigation strategies to reduce PTT methane emissions from time-fill CNG refueling stations.

To achieve the above objectives, the method and approach of this thesis work are to:

- Design and develop a measurement system to directly quantify methane mass emission rates from natural gas facilities;
- Validate and assess the performance, accuracy, and uncertainty of the developed measurement system.

1.4 Thesis Structure

This thesis is organized into five chapters. The overview of each chapter is outlined below.

- Chapter 1 introduces the background, motivation, objectives, and approach of this thesis work.
- Chapter 2 provides a review of methane emission measurement methods that can be applied to quantify methane emissions from natural gas facilities.
- Chapter 3 presents the design, component selection, and development of the high-volume system to quantify methane mass emission rates from natural gas facilities. Sensor calibration and system validation are discussed, and accuracy and uncertainty of the system are evaluated.
- Chapter 4 reports the field measurement results to quantify PTT methane emissions from the CNG fuel supply chain. A data set of component-level methane emissions for sources within a time-fill CNG refueling station, and methane emissions as percentages of station throughputs are presented. Abatement and mitigation strategies to reduce methane emissions from time-fill CNG refueling stations are also discussed.
- Chapter 5 describes the conclusions and recommendations for future research.

Chapter 2: Methane Emission Measurement Methods: Background Review

Methane emission measurements are conducted along a spectrum of spatial and temporal scales, from global annual assessments to instantaneous measurements of component emissions (Figure 2). Spatially, measurement methods are classified into top-down and bottom-up approaches. Temporally, measurements can be done over second, day, month, and year timescales [34].

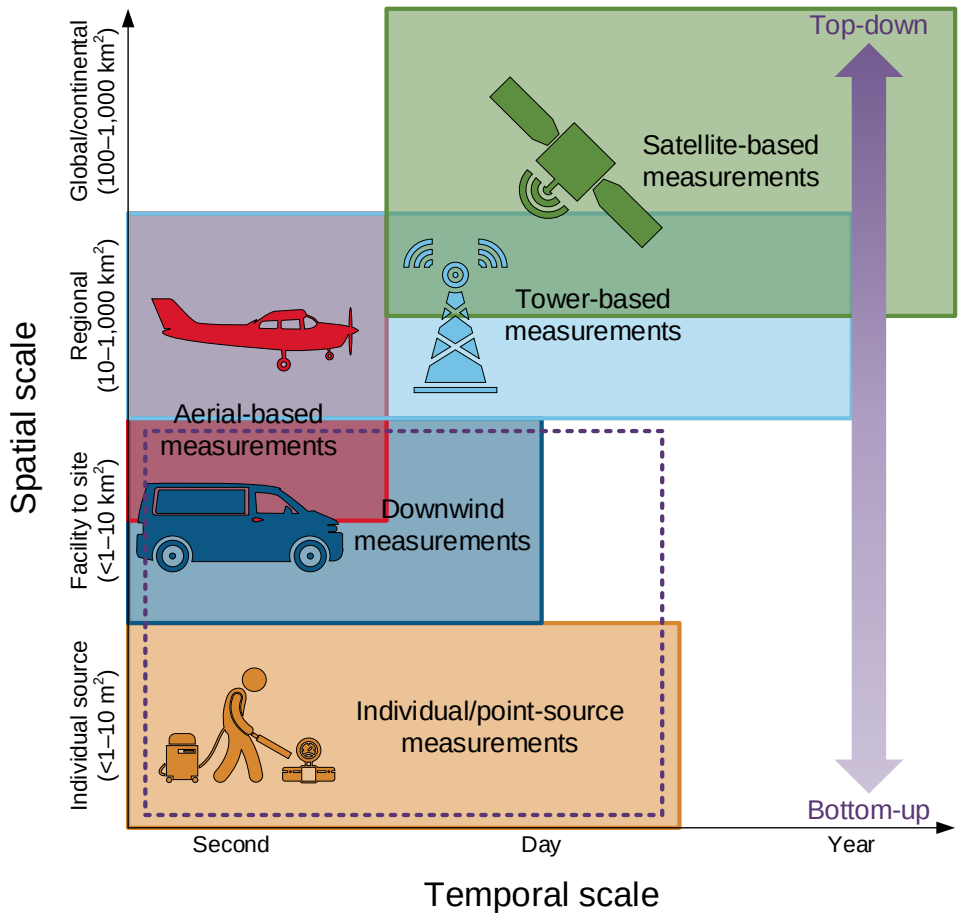

Figure 2. Methane emission measurements across a range of spatial and temporal scales.

Top-down approach aggregates emissions from multiple sources as a whole, while bottom-up approach extrapolates measurements from individual sources to estimate the total emissions at larger scales. As shown in Figure 2, top-down estimates at global, continental, and regional levels can be made by using satellite-, tower-, and aerial-based measurement methods. Bottom-up estimates at these levels can be constructed from site, facility, and individual emissions measured by using downwind and point-source measurements.

The dashed purple box in Figure 2 encompasses measurement methods that are applicable to create methane emission estimates at facility level. The top-down approach to measure the total methane emissions from a natural gas refueling facility includes aerial-based and downwind measurements. Although high-resolution methane-sensing satellites (i.e., TROPOMI and GHGSat) have recently been launched, current satellite-based measurements do not allow for facility-level estimations of methane emissions due to their low spatial resolutions [34,35]. Tower-based measurements are used to estimate methane emissions at the regional and city levels using a network of fixed sensors [34]. In the top-down approach, the facility emissions are measured as a whole [34]. In the bottom-up approach, emission factors, which are derived from measurements of individual components and single processes within the facility, are multiplied by facility activity data to estimate the total facility methane emissions [25,34]. The only bottom-up approach to facility-level emissions is point-source measurements.

In the top-down approach, facility emissions comprise contributions from all emission sources within the facility, including any unknown and inaccessible sources. However, this approach does not provide emission factors from particular sources or activities. Moreover, isolating a facility within the measurement area and disaggregating the measured emissions into

individual sources are difficult due to the sources being intermixed at the points of measurements [34].

In the bottom-up approach, facility-level emissions are granularized into emission factors, which are the necessary information for facility operators to mitigate emissions more effectively by targeting the sources. Additionally, the emission factor data can be combined with activity data and extrapolated to estimate the total methane emissions from similar facilities [34].

Table 1 provides a review on the various top-down and bottom-up methods that can be applied to estimate the total methane emissions from natural gas refueling facilities.

Table 1. Summary of methods for measuring methane emissions from a natural gas refueling facility.

Method	Advantages	Limitations	Status and references
Top-down approach to facility-level emissions			
Facility-scale aerial-based measurements	• Measures the total methane emissions remotely without the need of direct access to the facility [34,36].	• Requires appropriate meteorological conditions [34,36]. • Only applicable to high-emitting facilities due to the higher limits of detection than point-source measurements [34]. • Difficult to isolate the facility from closely-located sources [34,36].	Has been used to quantify methane emission rates from natural gas compressor stations (Lavoie et al. [37] and Nathan et al. [38]), gathering and boosting stations (Vaughn et al. [39]), gas processing plants and landfills (Lavoie et al. [37]), and flares (Gvakharia et al. [40]).
External tracer	• Measures the total methane emissions from a facility [26,34].	• Difficult to isolate facility if interfering sources are present [34,36].	Has been applied to quantify methane emission rates from natural gas compressor stations

	• Does not rely on theoretical modeling [26].	• Requires appropriate meteorological conditions [34]. • Prone to bias if tracer is at a significant distance from methane emission sources [34].	(Subramanian et al. [28]), gathering and boosting stations (Vaughn et al. [39]), gathering facilities and processing plants (Marchese et al. [27], Mitchell et al. [25], and Roscioli et al. [26]), and biogas plants (Fredenslund et al. [41]).
Inverse dispersion modeling	• Measures the total methane emissions remotely without the need of direct access to the facility.	• Difficult to isolate facility if interfering sources are present [34,36]. • Relies on models of meteorological conditions [34]. • Often results in estimates with significant uncertainties [34,36].	Has been used to estimate methane emission rates from well pads, compressor stations, gas processing plants, and landfills (Lan et al. [42]).

Bottom-up approach to facility-level emissions			
Point-source measurements	• Measures the total methane emissions from individual point sources [34].	• Requires an extensive number of individual measurements [34]. • Limited to measurements of safely accessible sources [34].	Has been applied to quantify emission rates from natural gas compressor stations (Subramanian et al. [28]), gathering and boosting stations (Vaughn et al. [39]), compressor stations and storage facilities (Johnson et al. [43]), biogas plants (Fredenslund et al. [41]), and CNG and LNG refueling stations (Clark et al. [19]).

2.1 Top-Down Approach to Facility-Level Emissions

2.1.1 Facility-Scale Aerial-Based Measurements

Aerial-based measurements can be applied at a wide range of spatial scales from global, continental, national, urban areas, specific oil- and gas-producing fields, and point or area sources. At the smallest scales, this approach can be used to target individual facilities and estimate the total methane emissions from point or area sources on the order of 10 – 100 m size [44,45].

The most common type of aerial-based measurements is the mass balance technique [45]. Figure 3 shows the schematic overview of the aerial-based mass balance technique. Methane concentrations at multiple altitudes on the downwind of the facility are measured such that the methane plume is captured on a two-dimensional vertical plane. Applying the Gauss's theorem and using the horizontal wind and methane concentration data, the flux of methane passing through the plane is calculated and the total emissions from the facility are estimated [36]. This technique was used to quantify methane emission rates from one compressor station and four gas processing plants in the Barnett Shale, US by Lavoie et al. [37], from a compressor station in the Barnett Shale, US by Nathan et al. [38], and from flares in the Bakken Shale, US by Gvakharia et al. [40].

The most recent development of the aerial-based mass balance technique was demonstrated by Conley et al. [45]. In this technique, an aircraft is flown at multiple altitudes circumscribing the target facility to create a virtual cylinder instead of a two-dimensional vertical plane [45]. This technique was used by Vaughn et al. [39] to quantify methane emission rates from natural gas gathering stations in the Fayetteville Shale, US.

The main advantage of the aerial-based approach is its capability to measure the total methane emissions remotely without the need of direct access to the facility. Emissions from multiple facilities within an area can also be measured in one flight. However, as measurements

are taken several kilometers downwind the facility, instrument with high enough sensitivity is required to measure methane concentrations above the background. Additionally, it is difficult to isolate the target facility from closely-located sources as multiple sources commingle at the concentration plane or cylinder generated by the flight paths. Aerial-based measurements also rely on favorable meteorological conditions and can be costly to deploy [34,36,45].

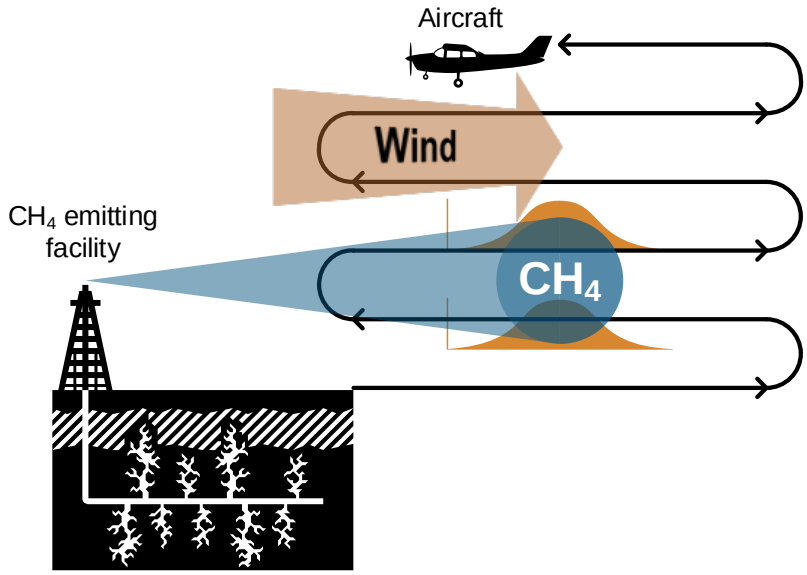

Figure 3. Schematic overview of the aerial-based mass balance technique.

2.1.2 External Tracer

Aggregate methane emissions from a facility with multiple emission sources can be quantified using the external tracer method [25,28,34]. Figure 4 shows the schematic overview of the external tracer method. In this method, a tracer gas is released at or near the emission source at a known flow rate. Simultaneous measurements of both methane and the tracer gas concentrations are taken across the plumes on the downwind, typically 0.5 to 3 km from the emission source using instruments in a mobile platform. Assuming that the methane and tracer

gases are collocated and undergo the same dispersion in the atmosphere, the methane emission rate can be calculated from the ratio of the concentrations of the two gases [26,34,36].

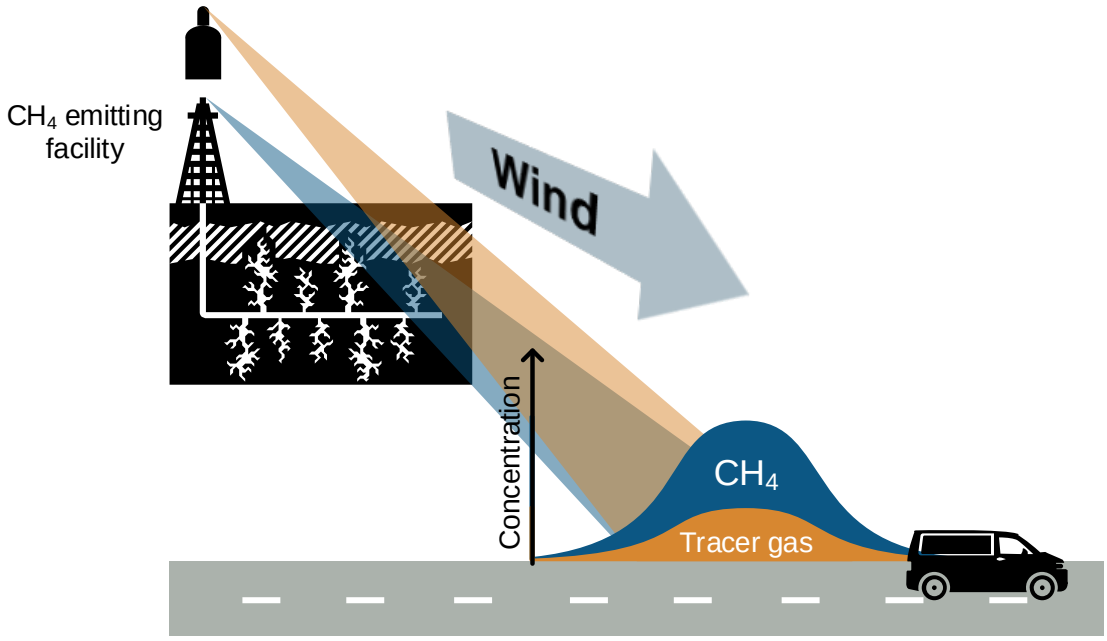

Figure 4. Schematic overview of the external tracer method.

A single tracer gas, such as sulphur hexafluoride, nitrous oxide, or acetylene, is traditionally used in the external tracer method [36]. Roscioli et al. [26] expanded the method and employed a second tracer to mitigate the situation where there is a separation distance between the tracer release point and the unknown emission source. The second tracer also provides internal standard and eliminates the need for additional instrument calibration.

Fredenslund et al. [41] used the single tracer gas method to quantify methane emissions from four biogas plants. Subramanian et al. [28] used the top-down dual tracer gas method to measure methane emissions from 45 compressor stations in 16 US states across the South, Mid-Atlantic, Northeast, Midwest, and Mountain West, and compared the results with those obtained using the bottom-up point-source measurements. The estimates from both measurements at most

sites were found to agree within experimental uncertainty. The dual tracer gas method was also used to measure facility-level methane emissions from 114 natural gas gathering facilities and 16 processing plants in 13 US states by Marchese et al. [25] and Mitchell et al. [27]. Vaughn et al. [39] used the method to quantify methane emissions from 14 natural gas gathering stations in the Fayetteville Shale, US and compared the results with those measured using the aircraft-based mass balance technique and point-source measurements combined with engineering estimates.

The external tracer is an established method to measure the total methane emissions from a facility. The main advantage of the method is that, it does not rely on theoretical modeling of gas dispersion, which is a complex function of wind speed and direction history, distance from the emission source, temperature, etc. [26]. When the methane and tracer gas plumes are fully mixed on the downwind, the analysis of the data is straightforward [36].

The external tracer method however requires appropriate meteorological conditions to ensure for sufficient mixing between the methane and tracer gases. The method relies on the correct placement of the tracer gas, as the results are prone to bias if there is a significant distance between the tracer release point and the unknown emission source. The presence of interfering methane sources can also cause significant errors in the total facility methane emissions [26,34,36].

2.1.3 Inverse Dispersion Modeling

The inverse dispersion modeling method can be used to measure the total methane emissions from a facility by taking downwind measurements of methane alone without a tracer gas. Downwind measurements can be taken dynamically (e.g., in a moving vehicle) to capture the methane plume, or at a stationary point. By feeding these measurement data into a dispersion

model, along with meteorological data such as wind speed, wind direction, and turbulence, the methane emission rate can be calculated [34,36].

Lan et al. [42] collected downwind methane concentrations data and meteorological parameters, and used the Gaussian dispersion model to estimate methane emissions from 125 well pads, 13 compressor stations, two gas processing plants, and 12 landfills in the Barnett Shale, US. Methane emissions from six of the compressor stations and one of the gas processing plants were also estimated using the Environmental Protection Agency AERMOD model. Uncertainty in the measurements were estimated using the Monte Carlo probabilistic uncertainty, and the results from both gas dispersion models agreed with each other within the measurement uncertainties [42].

The advantage of the inverse dispersion modeling over the external tracer method is that it measures the total facility methane emissions remotely without the need of direct access. However, as with the external tracer, it is difficult to isolate the total methane emissions from a facility if interfering sources are present. The inverse dispersion modeling method also requires desirable meteorological conditions, as high-quality data are critical as inputs to the models for emission estimates. Uncertainties in the estimates of emissions from dispersion models are usually significant [34,36]. For example, Lan et al. [42] reported that emission rates from compressor stations and gas processing plants had uncertainty bounds of −83/+295% for the Gaussian dispersion model and −37/+273% for the AERMOD model [42].

2.2 Bottom-Up Approach to Facility-Level Emissions

The only method in the bottom-up approach to facility-level emissions is point-source measurements. Point-source measurements can be applied to discrete emission sources that are well-defined. The methane emission rate at a point can be determined by measuring the

composition and flow rate of the gas at that point [34]. Many components in the natural gas supply chains (e.g. valves, flanges, connectors, reciprocating compressor rod packing, and vents) act as point sources.

The main advantage of point-source measurements is that it provides component-level granularity so that the sources can be targeted for emission reductions. However, point source measurements require an extensive number of individual measurements and are limited to safely accessible sources under normal operations [34].

Subramanian et al. [28] used point-source measurements to estimate site-level methane emissions from 36 compressor stations in the transmission system and nine compressor stations associated with underground storage facilities. Vaughn et al. [39] used direct measurements to generate methane emission rate estimates from natural gas gathering and boosting stations in the Fayetteville Shale, US. Fredenslund et al. [41] used on-site methods to quantify methane emissions from four biogas plants and compared the results with those obtained using the single tracer gas method. Johnson et al. [43] quantified methane emission rates from three natural gas compressor stations and two natural gas storage facilities using microdilution high-volume sampling (HVS) systems, and the same systems were used by Clark et al. [19] to quantify methane emissions from CNG and LNG refueling stations.

Methane emission estimates made from point-source measurements require a two-step process. First, all components within the facility are scanned to identify sources of leaks and emissions. Second, methane emission rates from all identified sources are measured directly [28]. These measurements are compiled to develop emission factors, i.e. emission rates per leak source. By multiplying these emission factors with activity data of the facility (e.g., the number of

refueling events), the total facility methane emissions can be estimated [34]. The details of each of the steps in point-source measurements are outlined in the following sections.

2.2.1 Emission Source Detection

Point-source measurements typically begin by performing a site inventory to identify all methane emission sources within the facility [46]. Components including flanges, unions, connectors, valves, valve stem packing, rod packing vents, open ended lines, pneumatic devices and controllers are checked for leaks [28,39]. Once detected, sources are identified and marked for emission rate quantifications.

The most widely used techniques for source detection are optical gas imaging cameras and handheld methane detectors. The former have the advantage of being capable to sense leaks from a distance without sampling the gas directly, and reach areas that are hard to access [41]. They can also screen a large number of components simultaneously, reducing the time required for source detection [43]. Subramanian et al. [28] performed source detection using a thermal gas imaging camera FLIR GasFindIR HSX (FLIR Systems, Inc., Wilsonville, OR, US). Vaughn et al. [39] employed optical gas imaging cameras FLIR GF320 (FLIR Systems, Inc., Wilsonville, OR, US) and Opgal EyeCGas (Opgal Optronic Industries Ltd., Karmiel, Israel), as well as a laser methane detector RMLD-IS (Heath Consultants Inc., Houston, TX, US) to locate emission sources. Fredenslund et al. [41] utilized optical gas imaging camera FLIR GF320 and portable methane analyzer EX-TEC PM 4 (Sewerin, Gütersloh, Germany) to locate emission sources within biogas plants. Johnson et al. [43] and Clark et al. [19] used handheld methane detectors Eagle II (RKI Instruments, Union City, CA, US) and an infrared camera FLIR GF-320 (FLIR Systems, Inc., Wilsonville, OR, US) for source detection. Other techniques for source detection include organic

vapor analyzers (OVAs), toxic vapor analyzers (TVAs), acoustic leak detectors, and soap bubble screening [47].

2.2.2 Emission Rate Quantification

A number of techniques can be employed for emission rate quantification. Fredenslund et al. [41] quantified methane leakages from digesters, biomass storage tanks, gas storage units, and ventilation units in biogas plants using the HVS technique. Methane concentration was measured using a photoacoustic gas monitor INNOVA 1412 (LumaSense Technologies, Ballerup, Denmark), laser gas detection module LGD F200 A CH4 (Axetris, Kaegiswil, Switzerland), or flame ionization detector with a non-methane hydrocarbon cutter 3-900 (J.U.M. Engineering, Bavaria, Germany). The flow rate of the biogas-air mixture was measured using a pitot tube/micromanometer ManoAir 100 (Schiltknecht, Gossau, Switzerland) or calculated from differential pressure across an orifice measured using a pressure sensor. Subramanian et al. [28] collected 1,398 individual direct measurements from component leaks (i.e. valves, flanges, connectors, open ended lines, etc.) and vented sources (i.e. reciprocating compressor rod packing, blowdown vents, centrifugal wet seals, etc.) using Bacharach Hi Flow Samplers (BHFSs) (Bacharach, New Kensington, PA, US) as the primary measurement devices, as well as acoustic emission instruments, anemometers, turbine flow meters, calibrated bags, and rotameters. Boom lifts, scaffolding, and extension poles were used to aid in quantifying emission sources at elevated heights. In the case of leaks or vents that could not be safely accessed, the average emission rates from the same components or leak types were used. Unburned methane emissions from engine and turbine exhausts were estimated using AP-42 emission factors [28].

BHFSs were also used by Vaughn et al. [39] as the primary devices for component-level measurements of flanges, unions, valve stem packing, rod packing vents, connectors, pressure regulators, tank vents, open ended lines, pneumatic devices, and controllers. Emissions from compressor engine crankcase vents and glycol dehydrator vents were estimated using Monte Carlo models. Unburned methane emissions from engine exhausts were estimated from the average emissions of representative engines [39].

Instead of using BHFSs, Johnson et al. [43] quantified methane emissions from natural gas compressor stations using HVS systems that they developed. The same systems were also used by Clark et al. [19] to quantify methane emissions from CNG and LNG refueling stations for heavy-duty vehicles. Details regarding the BHFS and HVS system are elaborated in the subsequent sections.

2.2.2.1 Bacharach Hi Flow Sampler

The BHFS was introduced in 2001 as a commercially available instrument to measure methane emissions in the natural gas industry. It has been used as the main instrument for measurement campaigns throughout the natural gas supply chain from production, processing, transmission, storage, to distribution [48,49].

The instrument generates a maximum suction flow rate of 17 m^3/h (10 scfm). The sampling hose, equipped with a variety of attachment options such as capture bag and flange strap, is placed adjacent to the point source to capture the entire natural gas leak along with surrounding air [48–50].

Methane mass emission rate is calculated from the volumetric flow rate of the captured natural gas-air mixture and methane concentration in the stream. Volumetric flow rate of the

captured natural gas-air mixture is determined by measuring pressure drop across an orifice. Methane concentration in the stream is measured using a catalytic oxidation sensor for concentrations between 0% and 5%, or thermal conductivity sensor for concentrations between 5% and 100% [48–50].

Although the BHFS is the primary instrument to measure methane emissions across the natural gas supply chain, it has a few of known limitations. The assumption that the BHFS completely captures the entire natural gas leak may not be valid due to the relatively low suction flow rate of the instrument. The instrument is also not methane specific and responds to heavier hydrocarbons in the natural gas [46]. The manufacturer of the BHFS claims that the instrument has an accuracy of ±10% [51].

Howard et al. [49] reported that, under certain circumstances, the BHFSs could fail to transition between the catalytic oxidation and thermal conductivity sensors to measure low and high methane concentrations, respectively. The failure was especially observed when the BHFS had not been calibrated for 2 weeks, used an out-of-date firmware, and was used for natural gas with methane content of less than 91%. This sensor transition failure can potentially result in erroneously low methane emission estimates.

2.2.2.2 High-Volume Sampling System

The HVS system was developed by a group of researchers out of West Virginia University led by Derek Johnson to overcome the limitations of the BHFS. Drawing on their expertise in automotive emissions testing, the HVS system design follows the principle of constant volume sampling for automotive emission certification [46]. The HVS system is portable and can be configured to be mounted on a cart, truck bed, or utility vehicle bed. It has been used to quantify

methane emissions from conventional and unconventional natural gas well sites, compressor stations, storage facilities, and CNG and LNG refueling stations [16,19,43,52–54].

The HVS system has a significantly higher flow rate than the BHFS, capable of drawing between 68 and 2,549 m^3/h (40 and 1,500 scfm) of air. It eliminates the interference of ethane, propane, and heavier hydrocarbons in the measurements, as well as the sensor transition failures, by using laser absorption spectroscopy instead of catalytic oxidation and thermal conductivity sensors. It is significantly more accurate than the BHFS with uncertainty of ±4.4% of the reading [46].

As mentioned in Section 1.3, two of the specific objectives of this thesis work are to quantify PTT methane emissions from time-fill CNG refueling stations and suggest abatement strategies for reducing the emissions. Almost all components within a CNG refueling station act as point sources. Point-source measurements allow for quantification of emissions from each of the sources and evaluation of their contribution to the overall PTT methane emissions. This information would provide data-driven insights to help station operators and regulators identify which sources could be targeted and prioritized for emission reductions. Additionally, the data for component-level emissions can be amalgamated into emission factors that can be used to estimate methane emissions from other refueling stations.

As per literature review, and analysis of the available point-source measurement technologies and their operating ranges and accuracies (BHFS [51] and the HVS system [46]), the HVS system is the most suitable method to achieve the objectives of this thesis work. The flexibility and underlying working principle of the system allow for accurate measurements of component-level methane emissions for sources within natural gas refueling infrastructure. The capability of the system to measure methane emissions from CNG and LNG refueling stations has

also been proven in the literature [16,19,46]. Details of the design and validation of the HVS system are presented in the subsequent chapter.

Chapter 3: Development of the High-Volume Sampling System

3.1 Design of the High-Volume Sampling System

The schematic of the HVS system is shown in Figure 5. The main components of the system include an inlet hose, damper, explosion-proof blower, outlet pipe, mass air flow (MAF) sensor, GHG analyzer, and a thermocouple. The specifications of the components are shown in Table 2.

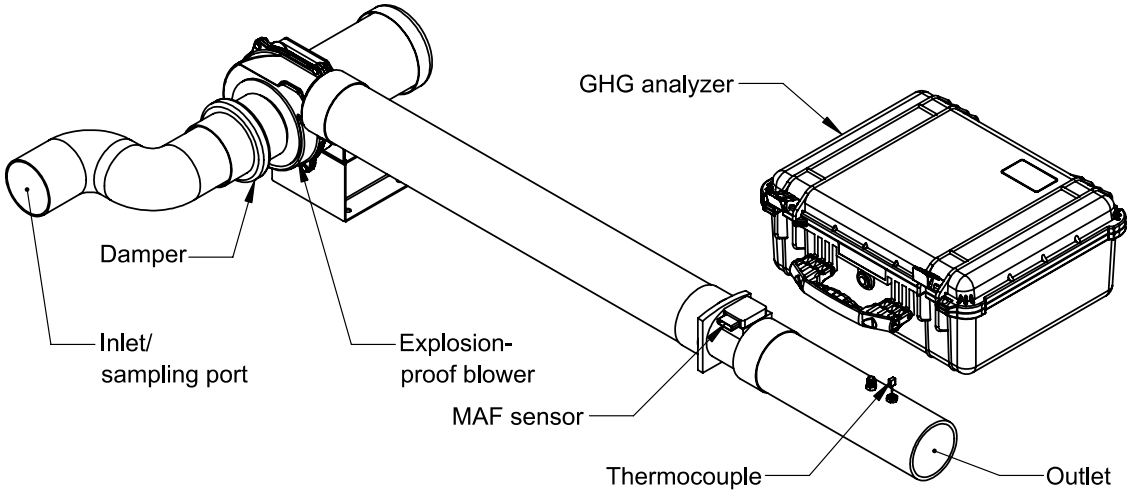

Figure 5. Schematic of the HVS system.

Table 2. Specifications of the components of the HVS system.

Component	Specifications
Inlet hose	Polyurethane dust-flex ducting Inner diameter: 102 mm Length: 3 m
Damper	Round duct iris damper Diameter: 102 mm
Explosion-proof blower	Airflow at 25.4 mm static pressure: 586 m^3/h
Outlet pipe	Standard-wall ABS pipe Inner diameter: 102 mm Length: 1.2 m

MAF sensor	Hot wire mass air flow sensor Repeatability: ±4% Outer diameter: 90 mm
GHG analyzer	Off-axis integrated cavity output spectroscopy Repeatability: ±2 ppb for methane, ±300 ppb for CO_2 Measurement range: 0 – 100,000 ppm for methane, 0 – 20,000 ppm for CO_2
Thermocouple	Type-T thermocouple Accuracy: ±1°C

The blower creates suction to capture the diluted natural gas leak and directs it into the sampling port. The damper is adjusted to control the flow rate and the mixing ratio of the natural gas-air mixture. The calibrated MAF sensor measures the standard volumetric flow rate of the natural gas-air mixture passing through the HVS system, and the GHG analyzer measures the concentration of methane in the natural gas-air stream.

The GHG analyzer quantifies methane, carbon dioxide, and water vapor concentrations based on the off-axis integrated cavity output spectroscopy (ICOS) technology [55]. Unlike the catalytic oxidation and thermal conductivity sensors that respond to the non-methane hydrocarbon components of natural gas [48], the GHG analyzer is methane specific. It provides higher accuracy and can measure methane concentrations between 0.01 and 100,000 ppm with repeatability of ±2 ppb [55].

The methane mass flow rate is determined using Eq. (1):

$$\dot{m}_{CH_4} = \dot{V}_{air}\, \rho_{CH_4} \left(C_{CH_4,out} - C_{CH_4,in}\right) \times 10^{-6} \quad (1)$$

where, $\dot{m}_{CH_4}$ is the methane mass flow rate (g/h), $\dot{V}_{air}$ is the standard volumetric flow rate of air (m^3/h), ρ_{CH_4} is the density of methane at standard condition (g/m^3), and $C_{CH_4,out}$ and $C_{CH_4,in}$ are

the exhaust and background methane concentrations (ppm). Measurements are conducted at atmospheric pressure, and temperature is continuously monitored using the thermocouple. Using these data, thermodynamic properties, e.g. density of methane, are calculated. It is assumed that the standard volumetric flow rate of the natural gas-air mixture is equal to the standard volumetric flow rate of air since the expected methane concentration in the flow passing through the HVS system is less than 5% (50,000 ppm).

After taking into account the pressure drop across the inlet hose, the HVS system is capable of drawing between 125 and 340 m^3/h of air. Given that the GHG analyzer can measure methane concentrations between 0.01 and 100,000 ppm, the methane mass emission rate that can be measured by the HVS system is between 0.000821 and 22,300 g/h. Final assembly of the HVS system is shown in Figure 6.

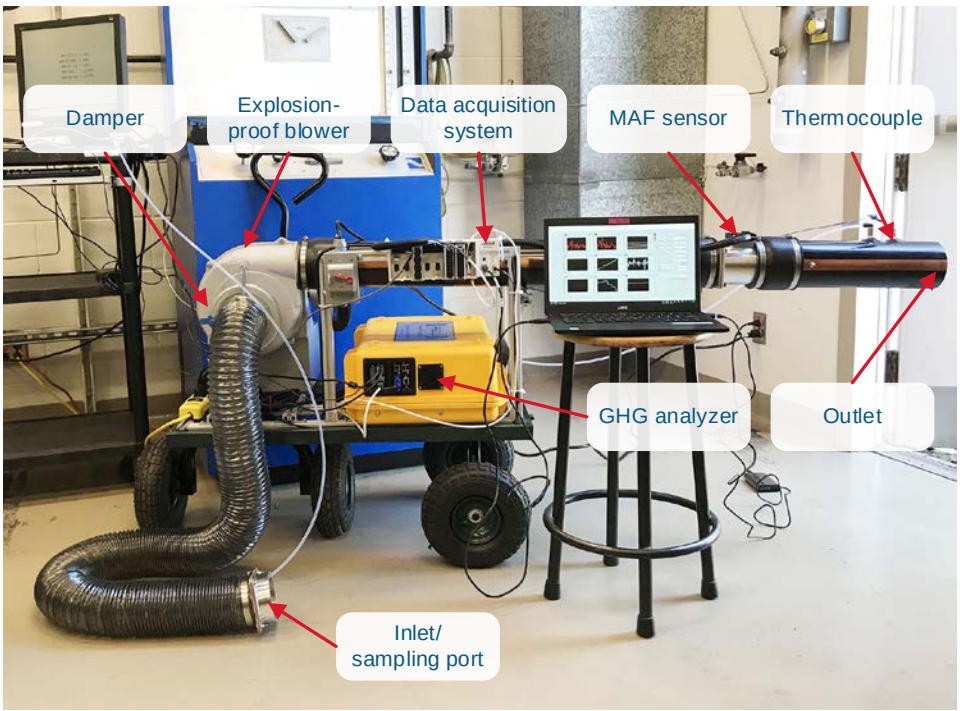

Figure 6. Final assembly of the HVS system.

3.2 Mass Air Flow Sensor Calibration

In order to measure the standard volumetric flow rate of the air stream, the MAF sensor was calibrated using an air flow bench of orifice plate-type with an accuracy of ±0.5%. Figure 7 shows the air flow rate passing through the HVS system as a function of MAF sensor voltage output. Error bars are not visible on the scale of the figure. A cubic curve is fitted on the calibration data set to correlate the MAF sensor voltage output, V_{MAF}, (V) to the air volumetric flow rate, $\dot{V}_{air}$, (m^3/h).

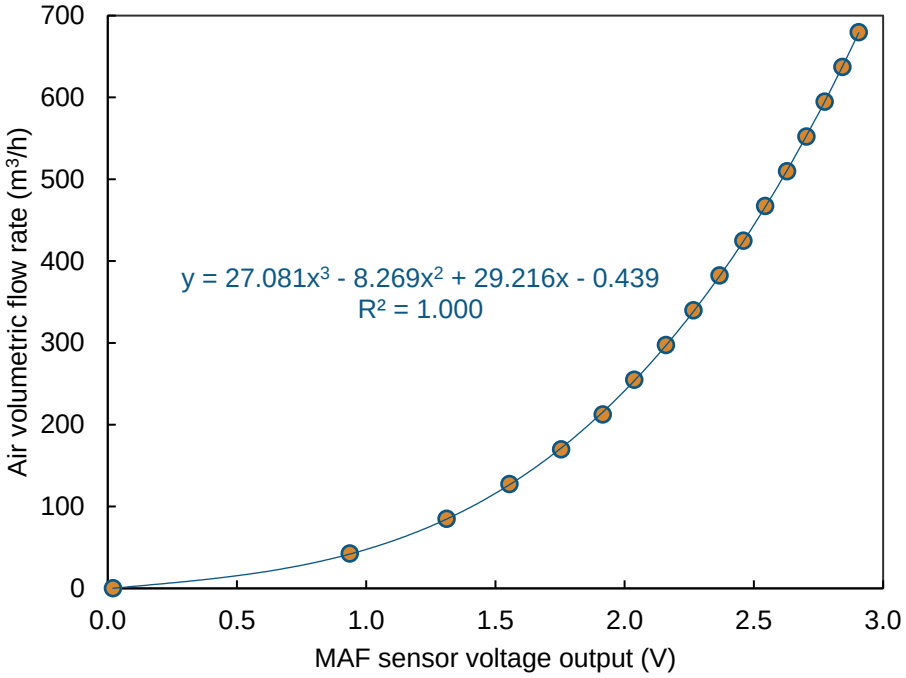

Figure 7. MAF sensor calibration curve.

Since the rated flow rate of the blower in the HVS system is 586 m^3/h, the MAF sensor calibration was performed for flow rates between 0 and 680 m^3/h. A stabilization period of 1 minute to ensure for steady-state condition, and data logging period of 2 minutes for each data

point were followed during the calibration process. As shown in Figure 7, the air volumetric flow rate is given by Eq. (2).

$$\dot{V}_{air} = 27.081\, V_{MAF}^3 - 8.269\, V_{MAF}^2 + 29.216\, V_{MAF} - 0.439 \quad (2)$$

3.3 Uncertainty Analysis

The methane mass emission rate, $\dot{m}_{CH_4}$, is calculated by Eq. (1). The volumetric flow rate of the air passing through the HVS system, $\dot{V}_{air}$, is obtained using the MAF sensor, and the exhaust and background methane concentrations, $C_{CH_4,out}$ and $C_{CH_4,in}$, are measured using the GHG analyzer. The combined uncertainty can therefore be determined using the law of propagation of uncertainty.

The percentage uncertainty in the volumetric flow rate of air, $u_{\dot{V}_{air}}$, is given by Eq. (3), and is a function of the MAF sensor repeatability, u_{MAF}, and air flow bench uncertainty, $u_{Flow\ Bench}$. The percentage uncertainty in the standard volumetric flow rate of air is therefore ±4.0%.

$$u_{\dot{V}_{air}} = \sqrt{u_{MAF}^2 + u_{Flow\ Bench}^2} \quad (3)$$

The uncertainty in the methane mass flow rate, $u_{\dot{m}_{CH_4}}$, is determined using the law of propagation of uncertainty, and is given by Eq. (4).

$$u_{\dot{m}_{CH_4}} = \left[\left(\frac{\partial \dot{m}_{CH_4}}{\partial \dot{V}_{air}} u_{\dot{V}_{air}}\right)^2 + \left(\frac{\partial \dot{m}_{CH_4}}{\partial C_{CH_4,out}} u_{C_{CH_4,out}}\right)^2 + \left(\frac{\partial \dot{m}_{CH_4}}{\partial C_{CH_4,in}} u_{C_{CH_4,in}}\right)^2\right]^{\frac{1}{2}} \quad (4)$$

Using Eqs. (1) and (4), the uncertainty in the methane mass flow rate measurements, $u_{\dot{m}_{CH_4}}$, can be expressed as follows:

$$u_{\dot{m}_{CH_4}} = \left[\left(\rho_{CH_4}\left(C_{CH_4,out} - C_{CH_4,in}\right) \times 10^{-6}\, u_{\dot{V}_{air}}\right)^2 + \left(\dot{V}_{air}\, \rho_{CH_4}\, u_{C_{CH_4,out}} \times 10^{-6}\right)^2 + \left(\dot{V}_{air}\, \rho_{CH_4}\, u_{C_{CH_4,in}} \times 10^{-6}\right)^2\right]^{\frac{1}{2}} \quad (5)$$

The uncertainty of the measured methane mass emission rate is ±4.0%. The dominating source of uncertainty is the uncertainty in the volumetric flow rate of the air stream measured by the MAF sensor. Uncertainty analysis for the air volumetric flow rate of 341 m^3/h, and exhaust and background methane concentrations of 37.407 and 1.951 ppm is shown in Table 3. The expected methane mass flow rate, $\dot{m}_{CH_4}$, is 7.94 ± 0.32 g/h.

Table 3. Uncertainty analysis for methane mass flow rate of 7.94 g/h.

Parameter	**Value**	u_{x_i} **(%)**	u_{x_i}
$\dot{V}_{air}$ (m^3/h)	341	4.0	14
$C_{CH_4,out}$ (ppm)	37.407		0.002
$C_{CH_4,in}$ (ppm)	1.951		0.002
ρ_{CH_4} (g/m^3)	656.88		
$\dot{m}_{CH_4}$ (g/h)	**7.94**	**4.0**	**0.32**

3.4 System Validation

Following the MAF sensor calibration, continuous leak and transient emission tests are required to validate the accuracy of the HVS system. The schematic of the test setup is shown in Figure 8. For safety reasons, validation tests were conducted using 4% methane-96% nitrogen gas mixture and 99.5% carbon dioxide.

In the continuous leak and transient emission tests, a mass flow controller (MFC), with 3.0 m^3/h (50 slpm) capacity calibrated for gases including methane and CO_2, was used to inject a known flow rate of gas from a cylinder into the HVS system. The outlet pressure of the gas cylinder was regulated at 138 kPag (20 psig) using a pressure regulator. The true flow rate or total mass of methane or CO_2 injected, as indicated by the MFC, was compared to the flow rate or total mass measured by the HVS system.

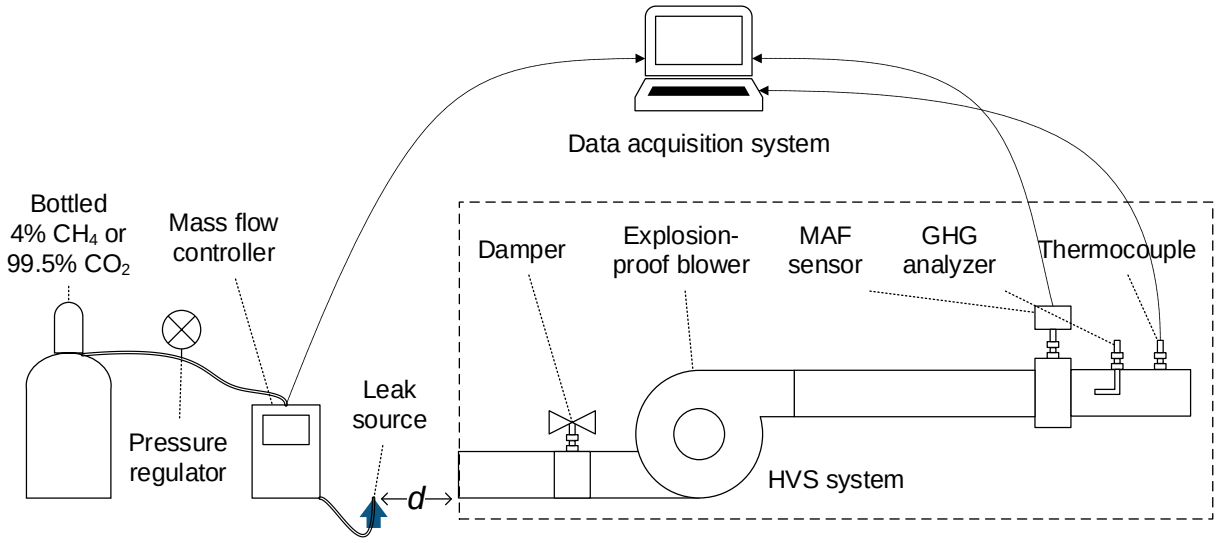

Figure 8. Schematic of the experimental setup for the continuous leak and transient emission tests. "*d*" and blue arrow show the distance and the direction of leak, respectively, in the continuous leak test with varying distance from leak source.

3.4.1 Continuous Leak Test

To validate the accuracy of the HVS system, continuous leak tests were conducted to simulate conventional steady-state leaks from the station components. Certain amounts of methane and CO_2 were injected using the MFC. The effects of varying the flow rate, and distance between the leak source and sampling port, on the accuracy of the HVS system were investigated. Methane was used in the test with varying flow rate, while the test with varying distance from leak source was conducted using CO_2. A stabilization period of 30 seconds to ensure for steady-state condition, and data logging period of 60 seconds were observed during the tests. Upon completion, the difference between the injected and measured methane or CO_2 flow rate was calculated and compared to the expected uncertainty.

Figure 9 shows a comparison between the actual methane mass flow rate set by the MFC and the methane mass flow rate measured by the HVS system. The background and injected methane concentrations measured by the GHG analyzer are 1.951 and 37.407 ppm, and the methane-air mixture volumetric flow rate measured by the MAF sensor are 341 m^3/h (Figure 9(a)).

Figure 9 shows delayed response to the change in methane concentration in the stream. This delay is characteristic of the GHG analyzer, which is mainly caused by the flow time passing through the measuring cell. The response time of the GHG analyzer includes dead time of 6.5 seconds and time constant of 7.0 seconds to reach 63% of its steady-state value. For conventional continuous leak, only the steady-state part of the data is considered and therefore the response time does not affect the measurements.

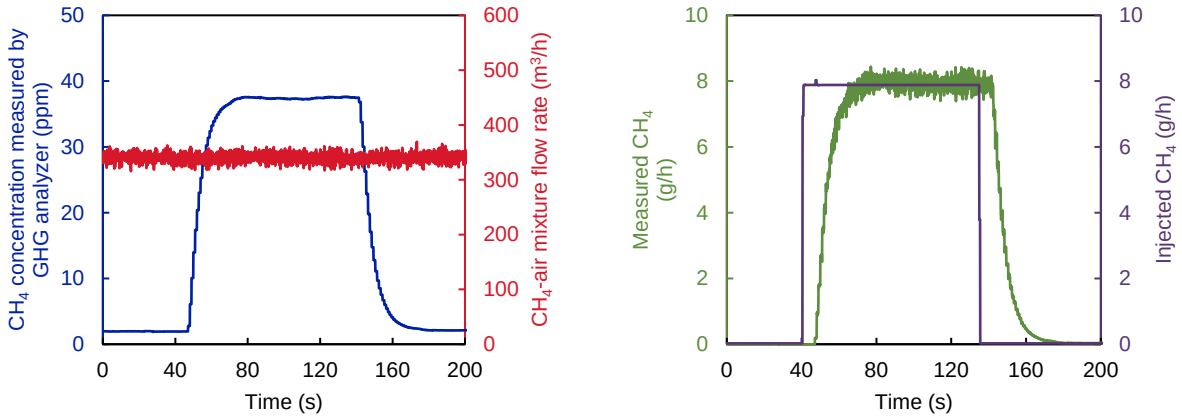

(a) (b)

Figure 9. (a) Methane concentration and the methane-air mixture volumetric flow rate measured by the GHG analyzer and the MAF sensor, respectively, and (b) a comparison of measured methane mass flow rate against the actual methane mass flow rate set by the MFC.

Following a similar calculation given by Eq. (1), the methane mass flow rate is calculated. Based on the HVS measurements, 7.94 g/h of methane is injected, which has 0.8% difference from the actual methane mass flow rate of 7.88 g/h set by the MFC (Figure 9(b)).

3.4.1.1 Continuous Leak Test with Varying Methane-Air Mixture Flow Rate

To test the accuracy of the HVS system for the range of expected steady-state emissions in the pump-to-tank segment of the natural gas fuel supply chain, the actual methane mass flow rate was varied from 7.88 to 78.8 g/h using the MFC. The averages of methane leaks from LNG and CNG stations are 12.80 and 35.69 g/h, respectively [19]. The methane-air mixture flow rate was also changed from 125 to 340 m^3/h. Figure 10 indicates that the HVS system measures the methane mass flow rate with maximum relative difference of 6.6% from the injected methane stream from the MFC.

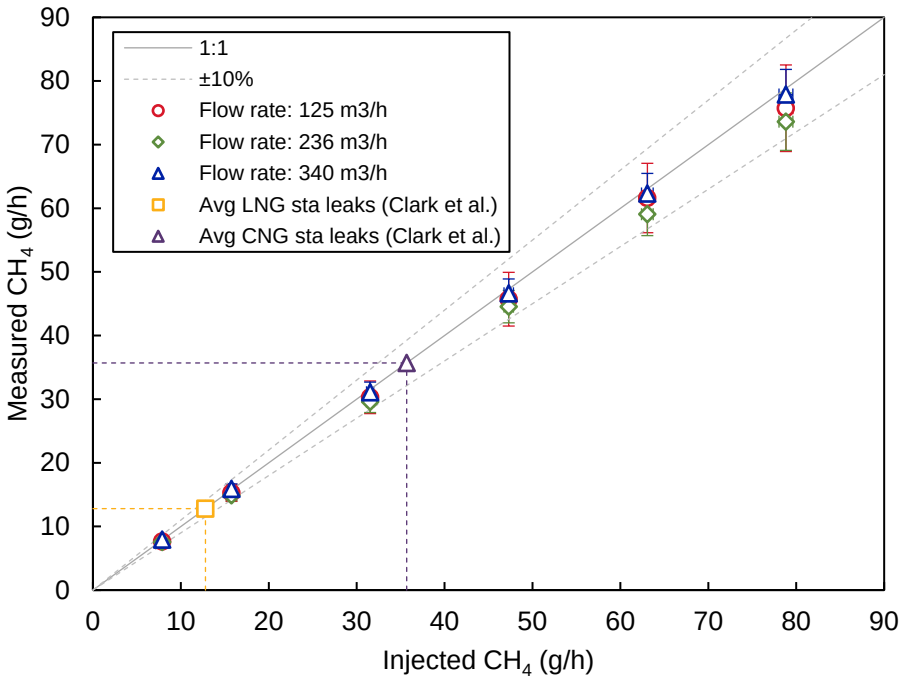

Figure 10. A comparison of measured methane mass flow rate by the HVS system and the actual methane mass flow rate set by the MFC.

3.4.1.2 Continuous Leak Test with Varying Distance from Leak Source

In the HVS method, it is important that the entire natural gas leak is captured by the system. In an ideal case, the HVS system sampling port coincides with the leak source and the jet of the leak is in the same direction as the suction of the system. Due to limitations in the actual natural gas facilities to get access to leak sources and environmental factors such as wind, there could be a distance separating the leak source and the HVS system sampling port. This distance (d) and the direction of leak were simulated in the test as shown in Figure 8. The test was conducted with direction of the jet of the leak perpendicular to the suction of the HVS system.

Figure 11 shows that varying the distance between the HVS system sampling port and the continuous leak source significantly impacts the CO_2 mass flow rate measurements. The results indicate that the HVS system can quantify CO_2 mass flow rates with ±10% accuracy as long as

the distance between the leak source and the HVS system sampling port is maintained at less than 50 mm. For longer distance of 100 mm, the measurement uncertainty dramatically increases to as high as ±83%.

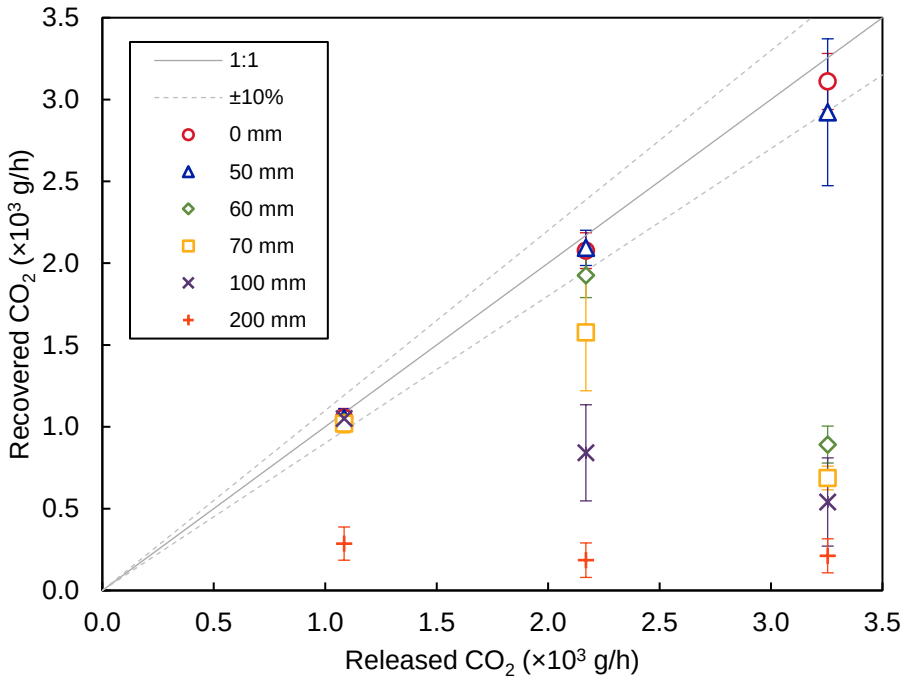

Figure 11. Effect of distance from the leak source on the CO_2 mass flow rate measurements of the HVS system. The actual CO_2 mass flow rate set by the MFC was varied from 1,085 to 3,254 g/h.

In such a case that there is a gap between the leak source and the HVS sampling port, a covering such as plastic sheeting should be used to enclose the source. Measurements should also be taken multiple times from various directions to ensure that all leak is captured by the HVS system.

3.4.2 Transient Emission Test

Transient emission test was conducted to simulate transient emissions, such as emissions from venting events or nozzle disconnects. Figure 12 shows an example of the time-series results of the transient emission test. Figure 12(a) shows the methane concentration and methane-air mixture volumetric flow rate measured by the GHG analyzer and the MAF sensor, respectively. As opposed to considering the steady-state part of the data and comparing the actual to measured flow rates (Figure 12(b)), the total mass of methane injected by the MFC is compared to the total mass of methane measured by the HVS system (Figure 12(c)). The total methane mass, m_{CH_4}, is determined using Eq. (6):

$$m_{CH_4} = \int_{t_1}^{t_2} \dot{V}_{air}\, \rho_{CH_4} \left(C_{CH_4,out} - C_{CH_4,in}\right) \times 10^{-6}\; d\tau \tag{6}$$

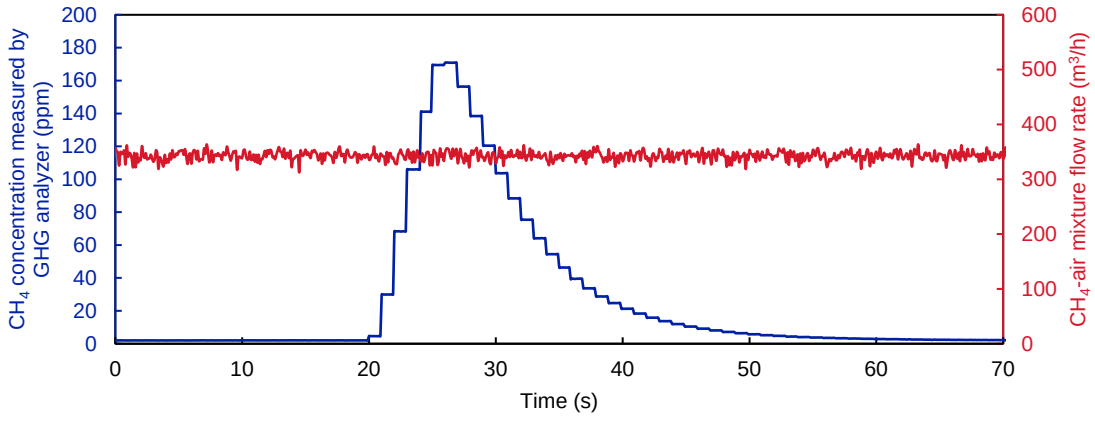

(a)

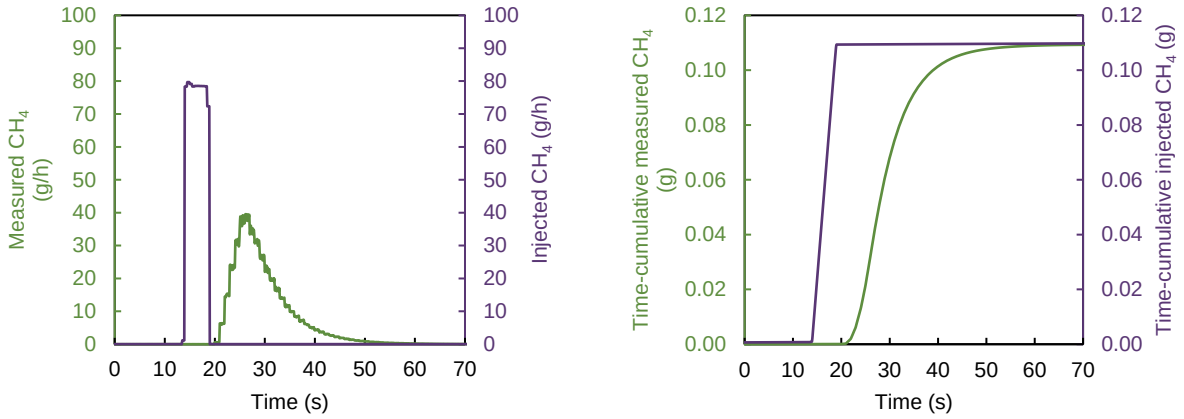

(b) (c)

Figure 12. (a) Methane concentration and the methane-air mixture volumetric flow rate measured by the GHG analyzer and the MAF sensor, respectively, (b) a comparison of the measured methane mass flow rate against the actual methane mass flow rate set by the MFC, and (c) a comparison of time-cumulative measured methane mass against the time-cumulative actual methane mass.

To test the accuracy of the HVS system to measure transient emissions in the pump-to-tank segment of the natural gas fuel supply chain, the total mass of methane injected by the MFC was varied by changing the duration of injection from 3 to 30 seconds. A constant injection rate of 0.0219 g/s, which is the maximum flow rate of the MFC for 4% methane, was applied throughout the test. Figure 13 shows that the HVS system is capable to quantify transient emissions with maximum relative difference of 6.6% from the injected methane stream from the MFC.

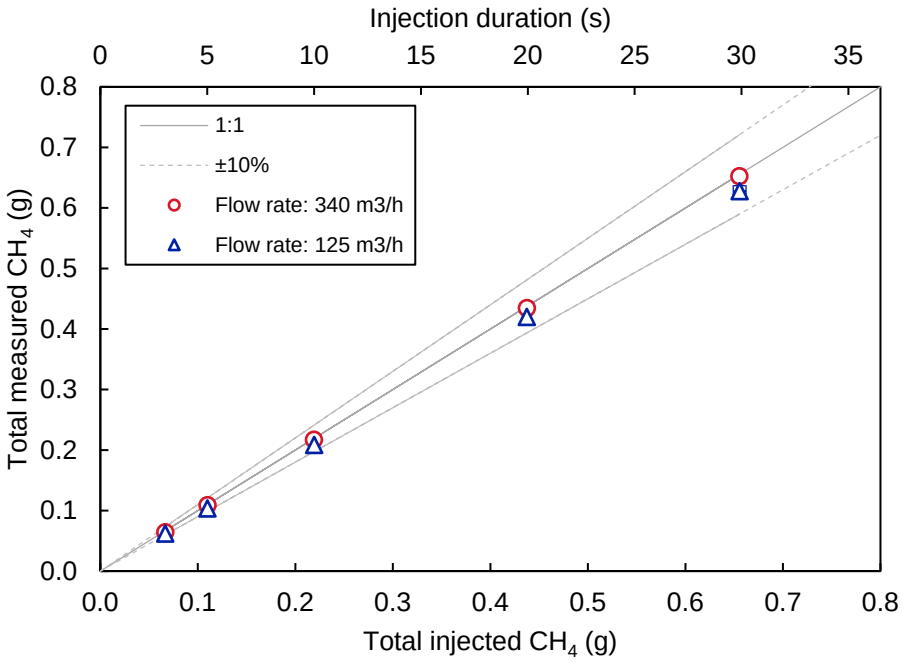

Figure 13. A comparison of measured methane mass by the HVS system and the actual methane mass set by the MFC under transient methane injections.

Chapter 4: Pump-to-Tank Methane Emissions from Time-Fill Compressed Natural Gas Refueling Stations

CNG refueling stations are designed and built unique to their applications. The size of equipment, such as compressors and storage tanks, and pressure outputs of the compressors are determined by the types of vehicles, demand or fleet size, and regional and national standards. The two general types of CNG refueling stations are fast-fill and time-fill [20].

Fast-fill CNG refueling stations are used for public retail applications. The vehicles arrive at the station at arbitrary times and are refueled from the on-site storage system, which usually consists of three vessels storing natural gas at pressures between 29.0 and 31.7 MPa (4,200 and 4,600 psi). Dispensing CNG from high-pressure storage system allows the vehicles to be refueled in short periods of time [19,20].

The time-fill is the most commonly used configuration of CNG refueling stations for private fleet applications, which run on set schedules and return to central locations after operations such as transit buses and refuse trucks. The vehicles are refueled directly from compressors for a period of several hours, commonly overnight when they are out of service and electricity prices are lower [19,20].

The PTT methane emissions from two time-fill CNG refueling stations were characterized in this study. The schematic of time-fill configuration of CNG refueling stations is shown in Figure 14. The sources of methane emissions from this segment include compressors, nozzle venting events, and nozzle disconnects, as well as continuous leaks from station components and nozzles during refueling processes.

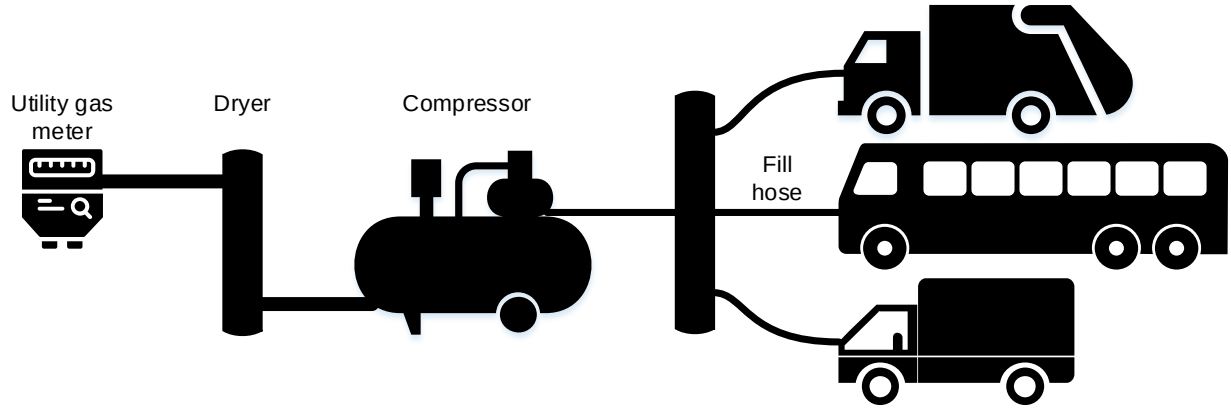

Figure 14. The schematic of a time-fill CNG refueling station.

4.1 Station Descriptions

The two CNG refueling stations characterized in this study represent the two extreme applications of time-fill configuration. Station no. 1 was constructed for small-scale consumer applications, while station no. 2 was commissioned for large fleet applications. Both stations are designed to fill 24.8 MPa (3600 psi) fuel systems.

Station no. 1 is a pilot-scale CNG refueling station providing fueling to three vehicles. The station utilizes a consumer-grade refueling system with maximum flow rate of 85 scmh (0.34 DGE/min or 50 scfm). The station system consists of two low-pressure dryers and two four-stage compressors, each enclosed in a single housing. Two fill hoses are attached to a post equipped with a vent stack. The total annual mass of natural gas supplied to the station was 21.8 tonne (t).

The vehicles in station no. 1 operate for 7 hours every working day. Two vehicles are filled in parallel and the nozzles are connected to the vehicle tanks until the following day. For 306 scm (75 DGE or 10,900 scf) CNG tanks, the time required to fill two tanks is at least 7.2 hours.

Station no. 2 is a CNG refueling station that provides fueling to a fleet of 57 vehicles. The facility is equipped with 16 hose posts with four fill hoses on each post. The station system utilizes

one low-pressure dryer and two separate four-stage compressors operating in parallel depending on the demand. The total annual natural gas supplied to the station was about 1.42 kilotonnes (kt).

The vehicles in station no. 2 operate for 10 hours every working day. The vehicles are filled in parallel for 14 hours until the following day, and the time required to fill all the tanks is at least 8 hours. As a simplification, it is assumed that the compressors on-site the facility operate for 12 hours every working day.

4.2 Emission Source Detection and Rate Quantification

The measurement campaigns were conducted at the two time-fill CNG refueling stations such that the normal operations of the stations were not disrupted. The measurement campaign at each station began by surveying all components and piping. Sources of emissions such as compressors and vent stacks were documented, and components and piping were scanned thoroughly for leaks using a Gas-Explorer handheld methane detector (Bascom-Turner Instruments, Inc., Norwood, MA, US). The handheld methane detector uses a catalytic sensor to detect concentrations of less than 5% (50,000 ppm) and thermal conductivity sensor to measure concentrations between 5% and 100%. It has a resolution of 20 ppm and accuracy of ±2% of reading ±20 ppm for concentrations below 40,000 ppm. For example, if the handheld sensor reads 10,000 ppm, the accuracy would be ±220 ppm (2% × 10,000 ppm ± 20 ppm). The response time of the instrument is 0.7 seconds [56].

The probe of the handheld methane detector was placed adjacent to the surface of the component and moved along the process flow of the refueling station. The probe was advanced along the peripheries of interfaces where leaks were more likely to be found. Locations of leak sources with methane detector readings of above 500 ppm were marked for later quantification.

The primary methane emission quantification method used in the measurement campaigns was the HVS technique. Methane emissions from compressors, component leaks, and nozzle leaks were treated as continuous leaks and quantified using the HVS system and method described in Section 3.4.1. Sampling port of the HVS system was placed on the location at which the highest methane concentration reading from the handheld methane detector occurred. Measurements were taken from different orientations and covering was used as needed to ensure that all the leaks were captured. Methane releases from nozzle venting events and disconnects are transient emission events and were quantified using the HVS system and method described in Section 3.4.2.

4.3 Component-Level Methane Emissions

4.3.1 Compressor Emissions

Each of the two compressor units in station no. 1 is contained in a separate housing. The compressor is controlled based on a simple logic in which it starts when sufficient pressure drop in the system is detected. Due to being inaccessible, all components of the compressor within the housing were treated as a single emission source. A plastic sheeting was used as an enclosure to seal off the housing and prevent natural gas from escaping. The sampling port of the HVS system was connected to a hole in the enclosure, and surrounding air was allowed to enter and dilute the natural gas through another opening.

Methane emissions from the compressor unit varied depending whether the unit was operating or idle, and during the cycling between on and off modes. Due to this variability, methane emissions from the compressor unit were measured continuously for a period of 30 minutes and the average was taken. Figure 15(a) shows the 32-minute methane concentration and methane-air mixture flow rate measured from one of the compressors in station no. 1. Using these

data, the methane emission rate of the compressor was calculated (Figure 15(b)). The emission rate varied between 0.9 and 35.7 g/h and averaged at 15.8 g/h with standard deviation of 6.6 g/h. Elevated level of emissions was observed when the compressor was switching between on and off modes.

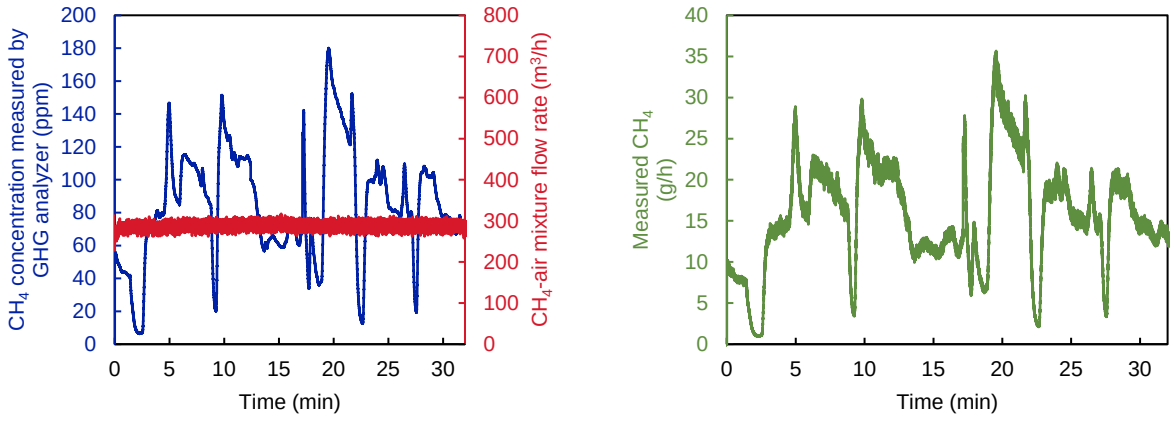

(a) (b)

Figure 15. Methane emission measurement data from one of the compressors in station no. 1: (a) methane concentration and methane-air mixture flow rate, and (b) methane emission rate.

The two four-stage reciprocating compressors in station no. 2 are contained in a single housing. Each compressor is equipped with a separate vent stack and louvers for air discharge. All components within the housing were treated as a single emission source, and emissions from the compressors were measured separately from the vent stacks and the louvers.

The sampling port of the HVS system was connected to the vent stack of the first compressor when it was on and off, and that of the second compressor when it was off. Figure 16(a) and (b) show the methane concentration and methane-air mixture flow rate, and the calculated methane emission rate, respectively, from the vent stack of compressor no. 1 in station no. 2 when the compressor was operating. Emissions from the vent stack of compressor no. 1 were

steady. Measurements from each of the two compressor vent stacks were taken for a period of around five minutes.

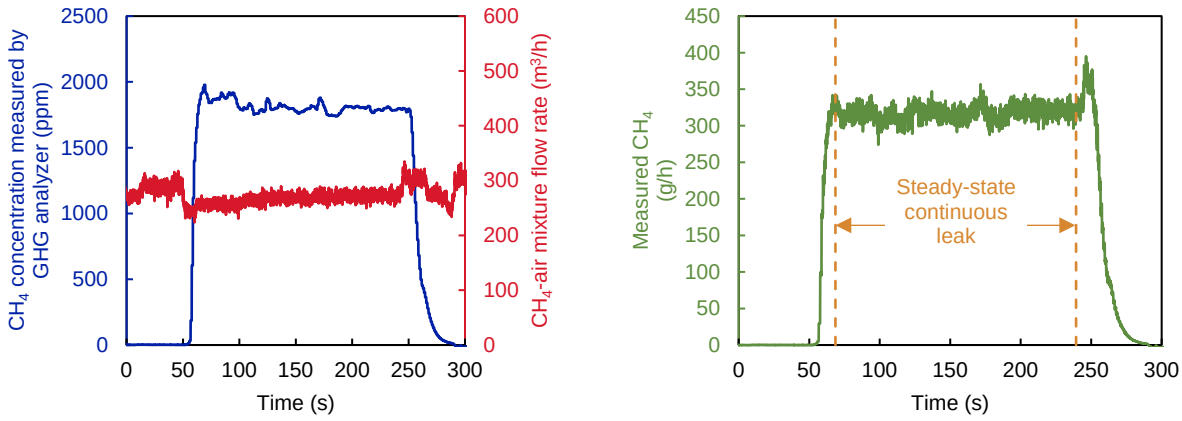

(a) (b)

Figure 16. Methane emission measurement data from the vent stack of compressor no. 1 in station no. 2 when the compressor was operating: (a) methane concentration and methane-air mixture flow rate, and (b) methane emission rate.

Methane emitted through the louvers of compressor no. 1 was quantified for around 13 minutes when the compressor was operating. During measurements, air discharge was only allowed through one of the louvers by closing the rest. Methane emission rate was quantified by measuring the velocity of the discharge air using an anemometer, and the concentrations of methane using the GHG analyzer. Measured methane emission rate from the louvers of compressor no. 1 in station no. 2 when the compressor was operating is shown in Figure 17.

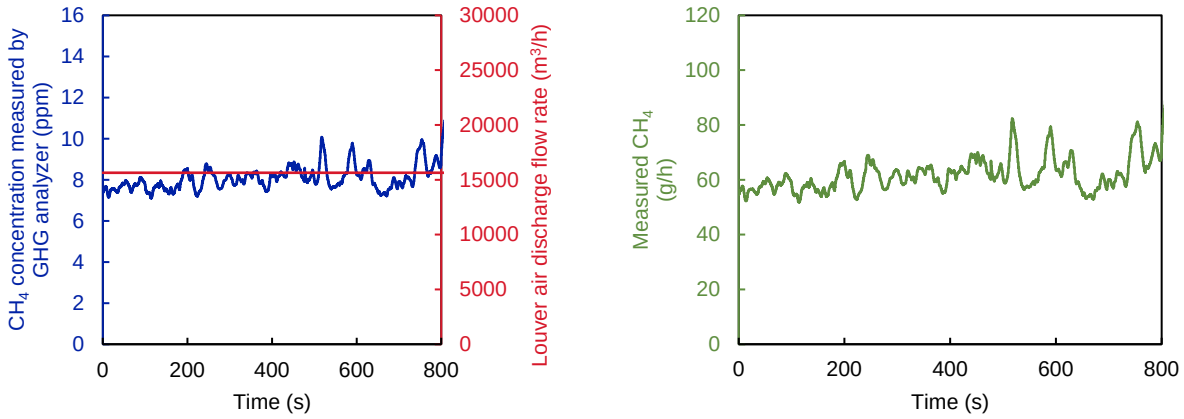

(a) (b)

Figure 17. Methane emission measurement data from the louvers of compressor no. 1 in station no. 2 when the compressor was operating: (a) methane concentration and methane-air mixture flow rate, and (b) methane emission rate.

The total methane emission rate from compressor no. 1 when it was operating is the sum of emissions measured from the vent stack and the louvers. Methane emission rate from compressor no. 1 varied between 326 and 439 g/h, and averaged at 379 g/h with standard deviation of 12 g/h when it was operating. When the compressor was off, the emission rate varied between 299 and 371 g/h, and averaged at 336 g/h with standard deviation of 10 g/h. Emissions from compressor no. 2 were measured when it was off only. The emission rate varied between 2.59 and 15.6 g/h, and averaged at 8.25 g/h with standard deviation of 2.81 g/h.

In the box-and-whisker plots shown in Figure 18–Figure 23, the band inside the box represents the average, and the box represents the average plus/minus standard deviation. The ends of the whisker represent the minimum and maximum of the data. As shown in Figure 18, compressor no. 1 in station no. 2 emitted up to 46 times as much methane as compressor no. 2. Emissions from compressor no. 1 when it was operating, and from compressor no. 2 when it was idle fall within the range of those reported by Clark et al. [19]. Emissions from compressor no. 1

when it was off were similar to those when it was on, and higher than those reported by Clark et al. [19].

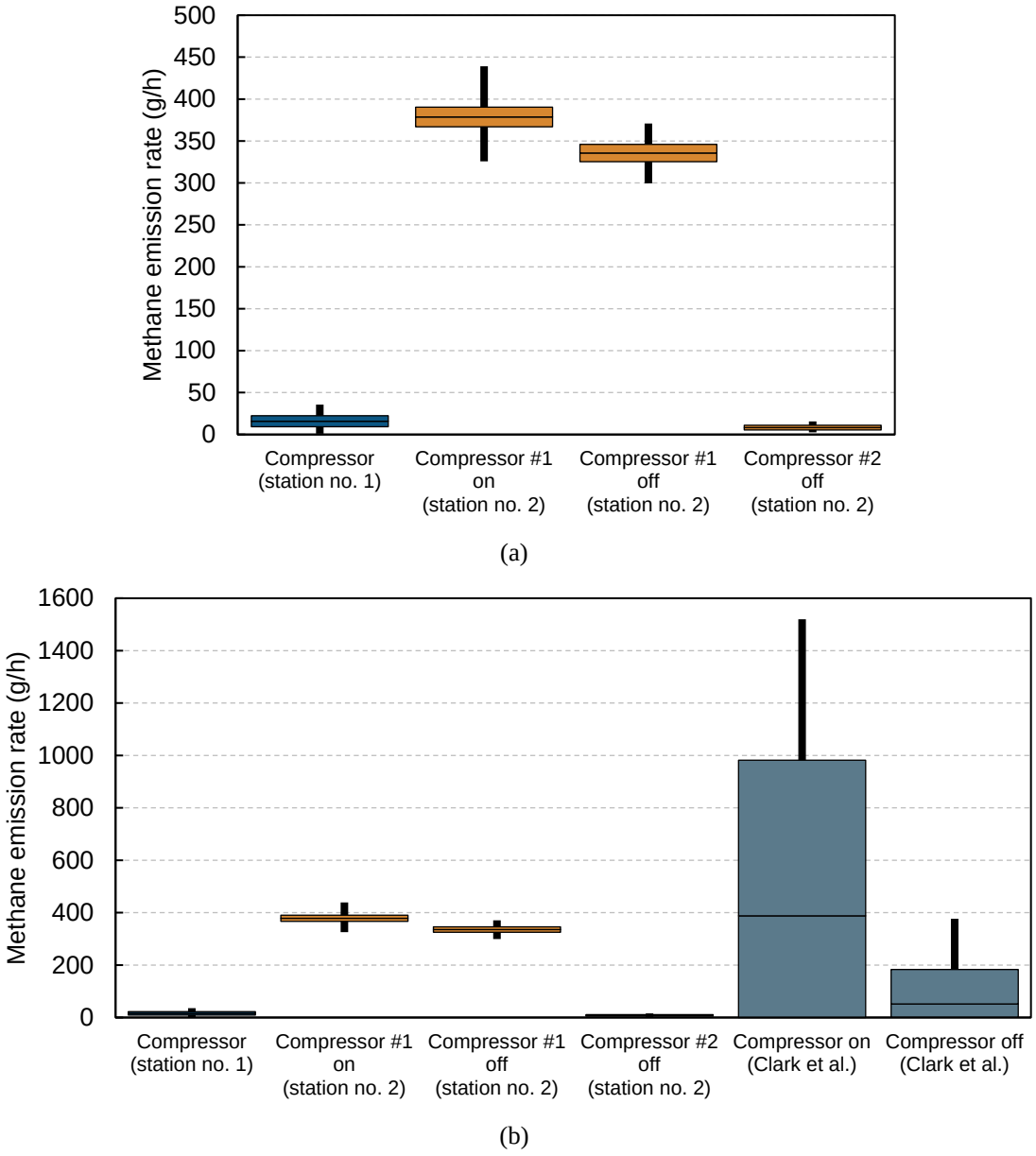

Figure 18. (a) Component-level methane emissions from the compressors in time-fill CNG refueling stations nos. 1 and 2, and (b) the comparison of results with the data reported from eight CNG refueling stations by Clark et al. [19].

4.3.2 Component Leaks

In station no. 1, one continuous leak was discovered on an electronically-actuated solenoid valve between the compressor units and the auxiliary fueling panel. The leak was quantified nine times when the station was operating, and four times when the station was idle. The leak ranged between 1.57 and 4.68 g/h, with average and standard deviation of 3.06 and 1.06 g/h, respectively.

In station no. 2, leaks were identified on the dryer drain valve, dryer tee fitting, and compression fitting on one of the hose posts. The minimum and maximum emissions were 0.74 and 1.18 g/h, respectively. Total emissions from the leaks averaged at 0.87 g/h with standard deviation of 0.06 g/h. Figure 19 indicates that the component leaks in stations nos.1 and 2 were on the low side, but comparable to those reported by Clark et al. [19].

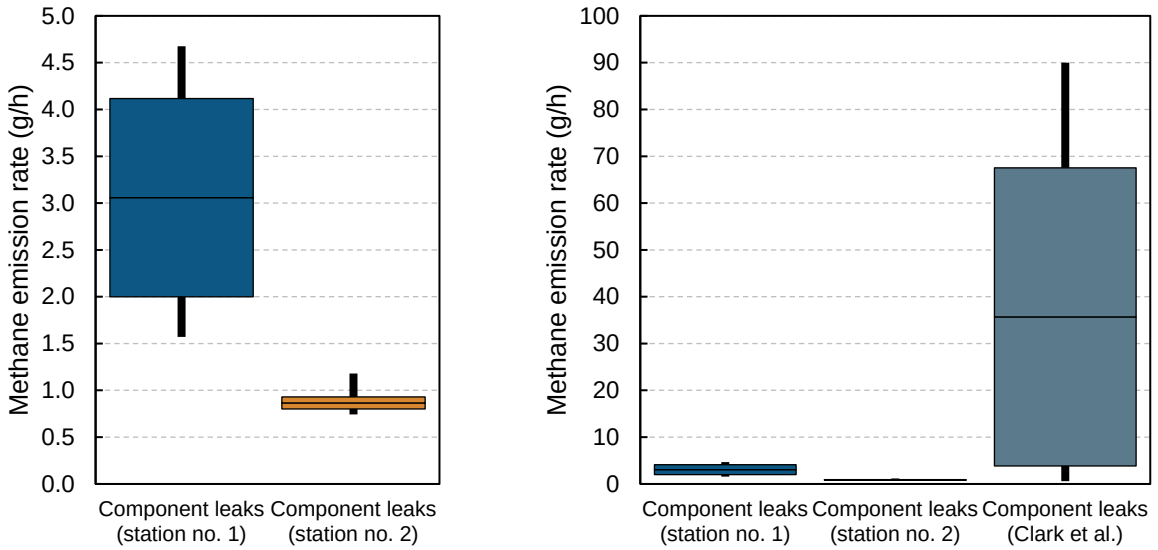

Figure 19. (a) Methane emissions from the component and piping leaks in time-fill CNG refueling stations nos. 1 and 2, and (b) the comparison of results with the data reported by Clark et al. [19].

4.3.3 Nozzle Leaks

In station no. 2, leaks were discovered on a large number of nozzles during the refueling process which was overlooked in the literature, e.g., Clark et al. [19]. This study for the first time discovered the significance of leak rates from specific type of nozzles during the time-fill refueling process. Station no. 2 employs nozzles with two different coupling designs. Out of the 57 nozzles in the station, 26 of them have the ball-lock design, and 31 nozzles employ the jaw-lock technology. Significant leaks were observed from the jaw-lock nozzles during refueling process, while ball-lock nozzles did not exhibit any.

Leaks from 12 jaw-lock nozzles were quantified in the measurement campaign. As shown in Figure 20, the average methane emission rate from jaw-lock nozzles was 33.4 g/h with standard deviation of 37.3 g/h. The minimum and maximum emission rates were 1.1 and 116.1 g/h, respectively. Component-level methane emissions from nozzle leaks in CNG refueling stations are unique to this study. No comparisons were made as there are no prior data sets in the literature.

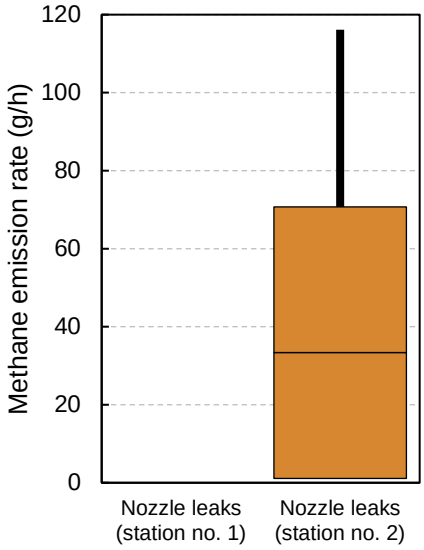

Figure 20. Component-level methane emissions from nozzle leaks in CNG refueling stations nos. 1 and 2.

4.3.4 Nozzle Venting and Disconnect Emissions

Prior to disconnecting the nozzle from a vehicle receptacle at the end of a refueling process, the nozzle and hose system is depressurized by venting the high-pressure natural gas remaining in the system. Both stations nos. 1 and 2 employ type 2 nozzles, in which the mechanism to operate the vent valve is external to the nozzle.

Station no. 1 uses a fill hose only. In station no. 1, the high-pressure natural gas left in the dead space volume between the receptacle check valve and the nozzle inlet valve, as well as in the fill hose between the nozzle and the auxiliary fueling panel, is vented through the same hose and to the vent stack.

Station no. 2 uses fill and vent hoses. In other words, two hoses are connected to a nozzle. In station no. 2, only the high-pressure natural gas left in the dead space volume between the receptacle check valve and the nozzle inlet valve is vented. Venting of this leftover natural gas is achieved through the use of a vent hose connected to the vent stack. Negligible amount of natural gas is emitted during the nozzle disconnection process in both stations.

Methane emissions from four nozzle venting events were quantified in station no. 1. Figure 21 shows the methane emission rate and time-cumulative methane emissions from a nozzle venting event in station no. 1.

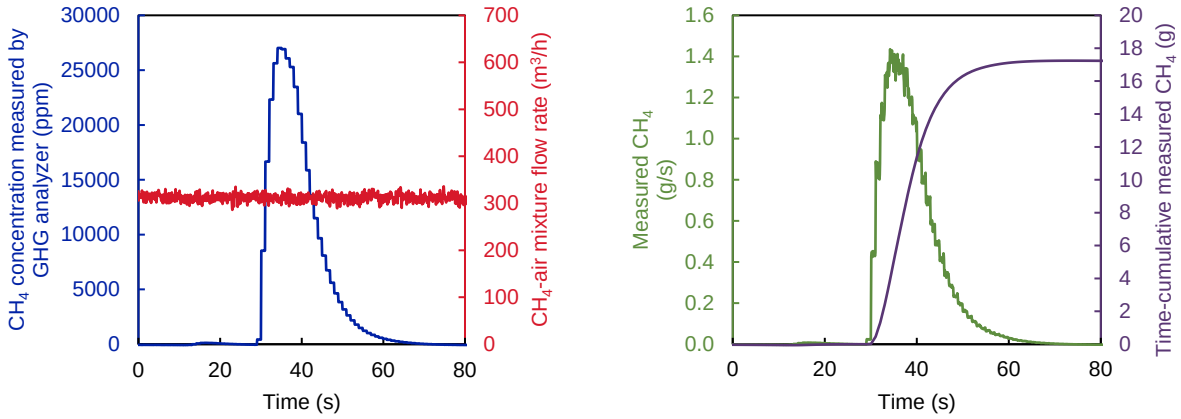

(a) (b)

Figure 21. Methane emission measurement data from a nozzle venting event in station no. 1: (a) methane concentration and methane-air mixture flow rate, and (b) methane emission rate and time-cumulative measurement.

In station no. 2, methane emissions from eight nozzle venting events were quantified at various refueling station system pressures as the measurements were taken premature of the completion of refueling processes. Figure 22 shows the methane emission data from the eight measured nozzle venting events. Using ideal gas law, the emissions were normalized to 24.8 MPa (3600 psi) as this is the pressure at which refueling process is complete.

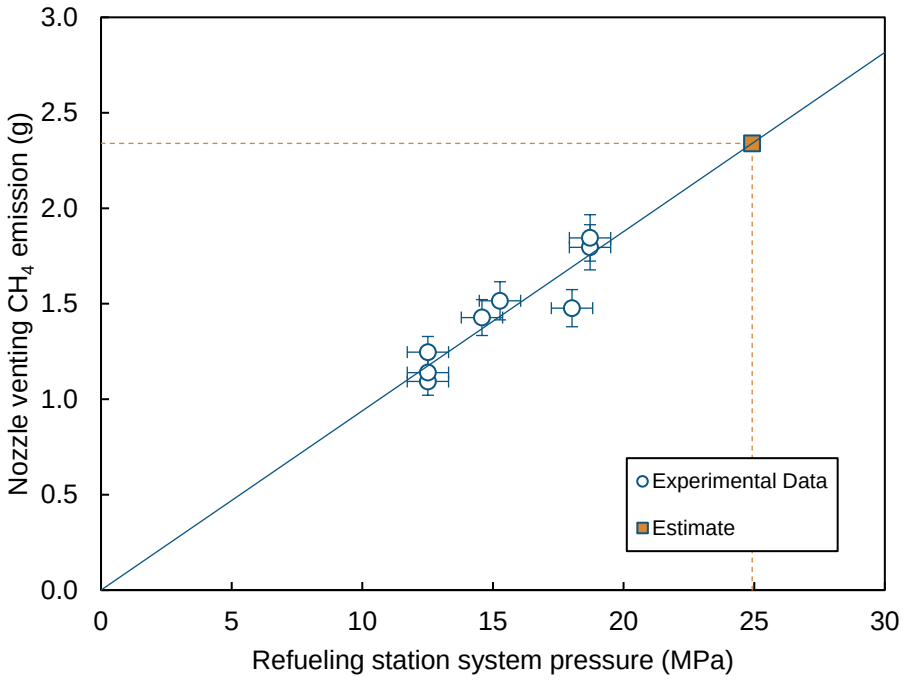

Figure 22. Methane emissions from eight nozzle venting events in CNG refueling station no. 2 at various refueling station system pressures and the estimated average nozzle venting emissions at 24.8 MPa (3600 psi).

As shown in Figure 23, the average nozzle venting emissions in station no. 1 were 17.2 g/event with standard deviation of 0.2 g/event. The minimum and maximum emissions were 17.0 and 17.4 g/event, respectively. It can be observed from Figure 23 that the measurements show higher values than those reported by Clark et al. [19]. The use of a single hose in station no. 1 results in a larger volume of high-pressure natural gas that needs to be vented following a refueling process. The average nozzle venting emissions in station no. 2 were 2.34 g/event with standard deviation of 0.16 g/event. The minimum and maximum emissions were 2.04 and 2.48 g/event, respectively. As shown in Figure 23, nozzle venting emissions from station no. 2 were at least seven times lower than those of station no. 1 and were within the range of those reported by Clark et al. [19].

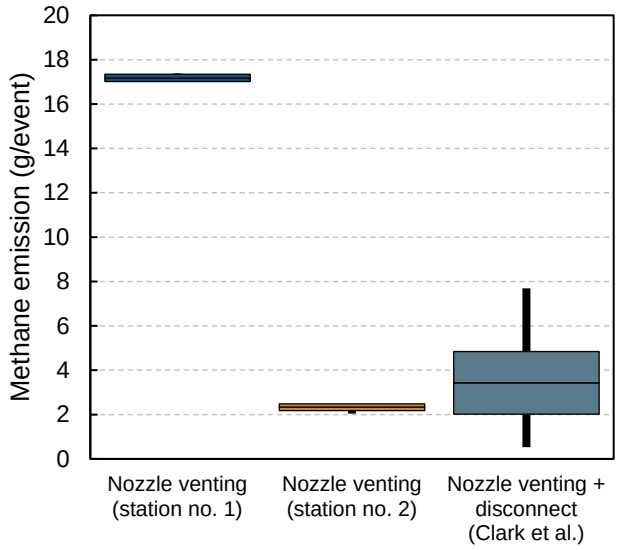

Figure 23. Component-level methane emissions from nozzle venting events in CNG refueling stations nos. 1 and 2, and comparison with the data reported by Clark et al. [19].

4.4 Pump-to-Tank Methane Emissions

Figure 24 shows the PTT system boundary of time-fill CNG refueling stations. The PTT methane emissions of CNG fuel can be calculated by dividing the annual methane emissions, which comprise component leaks, compressor emissions, nozzle venting emissions, and nozzle leaks, by the total natural gas supplied to CNG refueling stations.

The PTT methane emissions under the business-as-usual scenario were constructed using component-level emission data generated from the measurement campaigns. In the case of station no. 2, the data were collected prior to regularly scheduled maintenance of the station.

Uncertainties in the component-level methane emission rates were calculated at 95% confidence interval. Compressor emissions, component leaks, and nozzle leaks were treated as normal distributions, while nozzle venting emissions were treated as Student's t-distributions [57]. The contribution of each of the components to the annual methane emissions is expressed as a percentage based on central estimates (i.e., using the mean values).

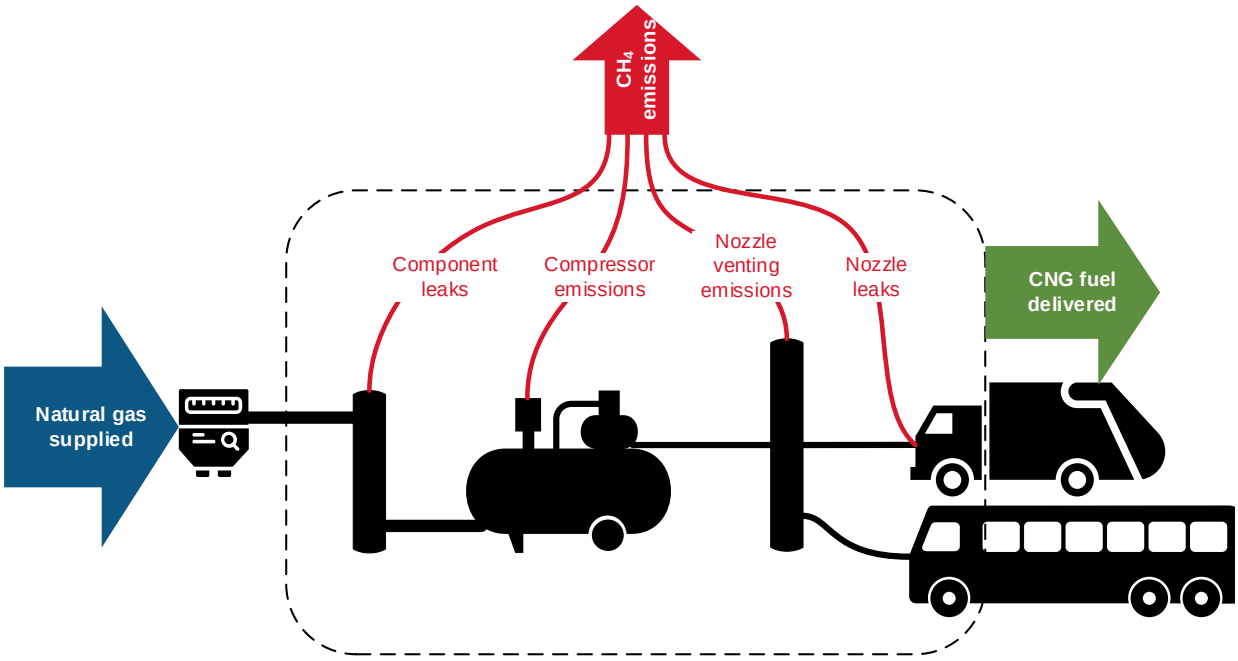

Figure 24. The PTT system boundary of time-fill CNG refueling stations.

As shown in Figure 25, the PTT methane emissions from CNG refueling stations nos. 1 and 2 under the business-as-usual scenario were 1.4 ± 0.8% and 0.7 ± 0.7%, respectively. The emission data from station no. 1 represent those of pilot or underutilized time-fill CNG refueling stations, whereas emission data from station no. 2 represent those of fully-operational time-fill CNG refueling stations.

Based on central estimates, the highest emitters in station no. 1 were the compressors, contributing 88.6% to the annual methane emissions. Component leaks and nozzle venting emissions contributed 8.5% and 2.9% to the annual methane emissions, respectively. In station no. 2, nozzle leaks and compressors were the most significant sources of methane emissions, contributing 66.6% and 32.9% to the annual emissions, respectively. Nozzle venting emissions and component leaks contributed 0.4% and 0.1% to the annual methane emissions.

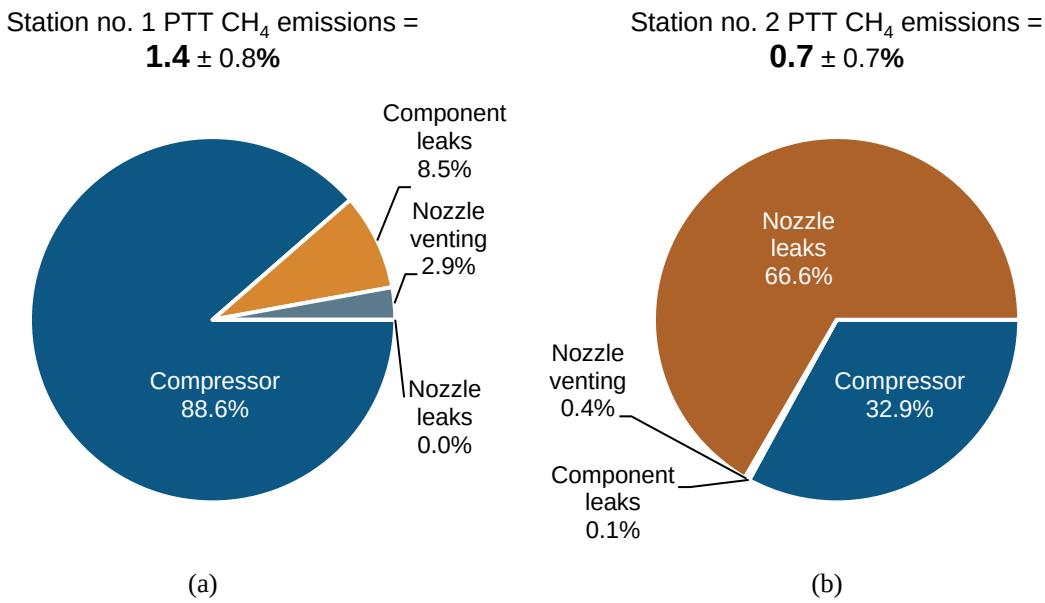

Figure 25. Breakdowns of the annual methane emissions from (a) station no. 1 and (b) station no. 2 by components based on central estimates under the business-as-usual scenario.

The breakdowns of the annual methane emissions from stations nos. 1 and 2 under the business-as-usual scenario are presented in Table 4 and Table 5, respectively. In station no. 1, the two compressor units emitted a total of 278 ± 173 kg of methane per year. This value represents 88.6% of the annual methane emissions from the station. As a consequence of the compressors starting when pressure drop is detected and working to maintain the pressure of the system, it was assumed that methane was emitted 24 hours a day even when the station was not operating. The methane emissions from component leaks were 3 ± 2 g/h, and no leaks were discovered from the nozzles in station no. 1. As the leaks occurred continuously, component leaks contributed 27 ± 14 kg or 8.5% to the annual methane emissions. The amount of methane released to the atmosphere from a nozzle venting event was 17.2 ± 0.6 g. As there were two vehicles filled in a day, the annual methane emissions from nozzle venting events were 9.0 ± 0.3 kg or 2.9% of the total.

Table 4. Breakdown of the annual methane emissions from station no. 1 as a percentage of the total natural gas supplied under the business-as-usual scenario.

	Methane emission rate								% of total CH_4 emissions
			Remarks	Working day		Weekend day		kg CH_4/yr	
				Freq./d	kg CH_4/d	Freq./d	kg CH_4/d		
Compressor	16 ± 13	g CH_4/h	2 compressors	24	0.8 ± 0.6	24	0.8 ± 0.6	278 ± 173	88.6
Component leaks	3 ± 2			24	0.07 ± 0.05	24	0.07 ± 0.05	27 ± 14	8.5
Nozzle leaks	0			24	0	24	0	0	0.0
Nozzle venting	17.2 ± 0.6	g CH_4/event		2	0.034 ± 0.001	0	0	9.0 ± 0.3	2.9
Total CH_4 emissions					0.9 ± 0.6		0.8 ± 0.6	313 ± 174	
Natural gas supplied								21,775	
Total CH_4 emissions/natural gas supplied								**1.4 ± 0.8%**	

In station no. 2, the nozzles of the jaw-lock design emitted 33 ± 73 g CH_4/h. As these 31 nozzles were connected for 14 hours a day on working days, and for 24 hours a day on weekend days, the annual methane emissions from nozzle leaks were 6,364 ± 10,038 kg. This amount represents 66.6% of the annual methane emissions from the station.

The second highest emitter in the station was the compressor units, contributing 3,147 ± 115 kg or 32.9% to the annual methane emissions. In this analysis, it was assumed that compressor no. 1 operated 12 h/day on working days. As emissions from compressor no. 2 were measured only when the unit was off, it was assumed that emissions from this compressor unit stayed constant.

The amount of methane released to the atmosphere from a nozzle venting event was 2.3 ± 0.4 g. As 57 vehicles were filled daily, the annual methane emissions from nozzle venting events were 35 ± 6 kg. This amount represents 0.4% of the annual methane emissions. Finally, the total emissions from component leaks were 7.6 ± 0.8 kg annually and represent 0.1% of the total methane emissions from station no. 2.

Table 5. Breakdown of the annual methane emissions from station no. 2 as a percentage of the total natural gas supplied under the business-as-usual scenario.

	Methane emission rate								% of total CH_4 emissions
			Remarks	Working day		Weekend day		kg CH_4/yr	
				Freq./d	kg CH_4/d	Freq./d	kg CH_4/d		
Compressor #1 on	379 ± 23	g CH_4/h		12	4.5 ± 0.3	0	0	1,186 ± 72	
Compressor #1 off	336 ± 20			12	4.0 ± 0.2	24	8.1 ± 0.5	1,889 ± 81	32.9
Compressor #2 off	8 ± 6			24	0.2 ± 0.1	24	0.2 ± 0.1	72 ± 37	
Component leaks	0.9 ± 0.1			24	0.021 ± 0.003	24	0.021 ± 0.003	7.6 ± 0.8	0.1
Nozzle leaks	33 ± 73		31 nozzles	14	14 ± 32	24	25 ± 54	6,364 ± 10,038	66.6
Nozzle venting	2.3 ± 0.4	g CH_4/event		57	0.13 ± 0.02	0	0	35 ± 6	0.4
Total CH_4 emissions					23 ± 32		33 ± 54	9,554 ± 10,039	
Natural gas supplied								1,423,727	
Total CH_4 emissions/natural gas supplied								**0.7 ± 0.7%**	

4.5 Discussion

Although the amounts of continuous methane emissions from component and piping leaks in both stations nos. 1 and 2 were not significant, periodic inspection and repair should be implemented by the station operators to completely eliminate these sources of emissions. With improvement in future technology, methane emissions from the compressor vent stacks and nozzle venting events can be reduced by routing the flows to a methane oxidizer.

The compressors in station no. 1 contributed 88.6% to the annual methane emissions. As mentioned in Section 4.3.1, the compressors start when the line pressure drops below a certain value. The compressors should ideally operate only when the nozzles are connected to the vehicle tanks at low pressures. However, component leaks downstream the compressors can cause sufficient pressure drop that triggers the compressors to run intermittently. To avoid undesired methane emissions from the compressors, the electronic modules can be programmed to operate the compressors manually or allow the compressors to run only between certain hours when the vehicles are docked in the station for refueling.

As opposed to the twin-hose assemblies used in station no. 2, single-hose design is used in station no. 1. In such design, depressurization of the entire hose as well as the dead space volume between the nozzle and vehicle receptacle are required following the completion of a refueling process. This results in nozzle venting emissions that are significantly higher than those from twin-hose assembly. In the case of stations nos. 1 and 2, nozzle venting emissions in station no. 1 were at least seven times as high as those in station no. 2.

Station no. 1 is a small-scale CNG refueling station that is currently used to fuel two vehicles in a day. Due to the low throughput of the station, the total methane emissions are significant relative to the total natural gas supplied. As the station system is capable of refueling four vehicles at a time, increasing the throughput of the station could potentially reduce the relative contributions of the compressor emissions and component leaks to the PTT methane emissions.

Under the minimal-emission scenario shown in Table 6, if the compressors were limited to operate for 15 hours during working days, component leaks were eliminated, twin-hose assemblies were employed, and the station throughput was increased to fueling four vehicles in a day, the PTT methane emissions from station no. 1 would decrease from current 1.4 ± 0.8% to 0.3 ± 0.2%.

Table 6. Breakdown of the annual methane emissions from station no. 1 as a percentage of the total natural gas supplied under the minimal-emission scenario.

	Methane emission rate								% of total CH_4 emissions
			Remarks	Working day		Weekend day		kg CH_4/yr	
				Freq./d	kg CH_4/d	Freq./d	kg CH_4/d		
Compressor	16 ± 13	g CH_4/h	2 compressors	15	0.5 ± 0.4	0	0	124 ± 101	98.1
Component leaks	0			24	0	24	0	0	0.0
Nozzle leaks	0			24	0	24	0	0	0.0
Nozzle venting	2.3 ± 0.4	g CH_4/event		4	0.009 ± 0.002	0	0	2.4 ± 0.4	1.9
Total CH_4 emissions					0.5 ± 0.4		0	127 ± 101	
Natural gas supplied								43,550	
Total CH_4 emissions/natural gas supplied								**0.3 ± 0.2%**	

In station no. 2, as nozzles of the jaw-lock design continuously leaked methane to the atmosphere during the refueling process, the most immediate and effective way to reduce emissions is to disconnect the nozzles from the vehicles during weekend days. Based on central estimates, this measure would reduce the annual methane emissions by 3 t. Replacing the leaking nozzles would completely eliminate leaks from the nozzles during the refueling process and reduce the annual station emissions by 6 t. Periodic inspection for nozzle leaks should be implemented along with replacement of the nozzles that have reached the end of useful life.

Following the inspection of compressor no. 1 in station no. 2 that emitted up to 46 times as much methane as compressor no. 2, it was found that one of the drain valves in the compressor system was not fully closed. This release of undesired methane emissions could have easily been mitigated by implementing a regular inspection program. By keeping emissions from compressor no. 1 as low as those of compressor no. 2, the annual station emissions could have been reduced by 3 ± 14 t.

Upon communicating these findings with the station operators, recommendations to reduce methane emissions from station no. 2 were implemented in the following regularly scheduled maintenance of the station. The leaking nozzles were replaced, and the root cause of abnormal emissions from compressor no. 1 was fixed. Under the minimal-emission scenario shown in Table 7, if compressor emissions were kept at a minimum, and component and nozzle leaks were eliminated, the PTT methane emissions from station no. 2 could potentially be reduced from current 0.7 ± 0.7% to 0.013 ± 0.003%.

Table 7. Breakdown of the annual methane emissions from station no. 2 as a percentage of the total natural gas supplied under the minimal-emission scenario.

Methane emission rate									% of total CH_4 emissions
			Remarks	Working day		Weekend day		kg CH_4/yr	
				Freq./d	kg CH_4/d	Freq./d	kg CH_4/d		
Compressor #1 on	8 ± 6	g CH_4/h		12	0.10 ± 0.07	0	0	26 ± 17	
Compressor #1 off	8 ± 6			12	0.10 ± 0.07	24	0.2 ± 0.1	46 ± 22	80.6
Compressor #2 off	8 ± 6			24	0.2 ± 0.1	24	0.2 ± 0.1	72 ± 37	
Component leaks	0			24	0	24	0	0	0.0
Nozzle leaks	0		31 nozzles	14	0	24	0	0	0.0
Nozzle venting	2.3 ± 0.4	g CH_4/event		57	0.13 ± 0.02	0	0	35 ± 6	19.4
Total CH_4 emissions					0.5 ± 0.2		0.4 ± 0.2	179 ± 47	
Natural gas supplied								1,423,727	
Total CH_4 emissions/natural gas supplied								**0.013 ± 0.003%**	

Compressors in both CNG refueling stations nos. 1 and 2 are significant contributors to the PTT methane emissions. Several best practices can be implemented by the station operators to minimize methane emissions from the compressors in time-fill CNG refueling stations. First, abnormal levels of emissions can be identified if a regular inspection program is in place. Diagnosis can subsequently be carried out and actions can be taken to eliminate the root cause of elevated levels of emissions. Second, limiting operations of the compressors to certain hours when the vehicles are docked, using a buffer tank to maintain the pressure of the system, and implementing a robust startup logic can prevent the compressors from running unintentionally and producing undesired methane emissions. A buffer tank can also be used to refuel a small number of vehicles outside the scheduled time. Finally, low-emission blowdown strategies can be implemented to minimize the amount of methane emitted to the atmosphere during compressor shutdown. The natural gas that is vented during a blowdown or depressurization following a shutdown can be recovered by routing it to a storage tank and recompressing it in the following

cycle. The compressor system can also be maintained at high pressure following a shutdown to prevent the release of methane to the atmosphere.

As mentioned in Section 4.3.1, measurements from the compressor vent stacks and louvers in station no. 2 were taken for periods of around five and 13 minutes, respectively, when compressor no. 1 was on and off. As a result, temporal emission variations that occur due to events such as blowdown during compressor shutdown were not captured. In addition, methane emissions from compressor no. 1 after the open drain valve was closed were not quantified. Due to the limited sample size of the data collected, more measurements are needed to increase the confidence level of the data.

The measurement data from two time-fill CNG refueling stations presented in this chapter demonstrate the successful utility of the HVS system to quantify PTT methane emissions from the natural gas refueling infrastructure. The portability and flexibility of the HVS system allowed for measurements of various point sources at natural gas refueling facilities in different locations. Component-level methane emissions were obtained with degree of accuracy that is within the experimental uncertainty of the measurements.

The study conducted by Clark et al. [19] is the only published data in the literature on the PTT methane emissions of natural gas refueling stations. The results of component-level methane emissions from time-fill CNG refueling stations obtained in the present study can be concatenated with the published data to build a more robust database of component-level methane emissions from natural gas refueling infrastructure. Ultimately, these data can be used in the future to develop emission factors for building life cycle assessments of natural gas fuel and comprehensive greenhouse gas inventories.

The average PTT methane emissions from the two time-fill CNG refueling stations studied in this thesis were 1.1 ± 0.5%. Given that WTW methane leakage (e.g., 2.4% in the case of LNG fuel in Canada [21]) dictates the environmental performance of natural gas as a transportation fuel, it is uncertain whether natural gas is a net GHG reducer as compared to diesel. Future LCA studies should incorporate methane emissions from this otherwise overlooked segment to determine the effectiveness of using natural gas in cutting transportation GHG emissions in the near- to medium-term.

Chapter 5: Conclusions and Future Work

5.1 Conclusions

The overall goal of this work was to quantify PTT methane emissions from natural gas refueling infrastructure. Among the methods that can be applied to estimate the total methane emissions from natural gas refueling facilities such as aerial-based measurements, external tracer method, and inverse dispersion modeling, point-source measurements are the most appropriate method to achieve the objectives of this thesis. Component emission data generated by point-source measurements provide useful information for facility operators and regulators to identify which sources should be targeted for emissions reduction.

The methodology of this thesis involved the development of the HVS system to perform point-source measurements at natural gas refueling stations. Compared to the commercially available instrument to measure methane emissions across the natural gas supply chain, the HVS system offers a wider range of measurements and higher accuracy, while maintaining the portability and flexibility features.

The HVS system works by creating suction to capture natural gas leak through its sampling port. A MAF sensor measures the volumetric flow rate of the natural gas-air mixture, and a GHG analyzer quantifies the concentration of methane in the stream. Calibration of the MAF sensor was performed against an air flow bench to obtain the correlation between the MAF sensor output voltage and the air volumetric flow rate.

The performance of HVS system was validated by conducting continuous leak and transient emission tests to simulate conventional steady-state component leaks and transient venting emissions, respectively. Known mass flow rates of methane or CO_2 were injected into the

sampling port and compared to the readings of the HVS system. The continuous leak and transient emission tests with varying methane-air mixture flow rate showed that the HVS system measured methane emission rate and total methane emissions with maximum uncertainty of 6.6%. The continuous leak test was also conducted with varying distance from the simulated leak source. The results suggested that, in the case that there is a gap between the leak source and the HVS sampling port, an enclosure should be used and measurements should be taken multiple times from various directions to ensure that all natural gas leak is captured by the HVS system.

The utility of the HVS system was successfully demonstrated at two time-fill CNG refueling stations to generate a data set of component-level methane emissions. Station no. 1 is of pilot scale, and station no. 2 is a fully-operational station. The HVS system was used to measure methane mass emission rates from compressors, component and nozzle leaks, and nozzle venting events. Based on central estimates, the results showed that natural gas compressors were a significant source of emissions in station no. 1, contributing 88.6% to the annual methane emissions. Prior to regularly scheduled maintenance, compressor emissions and nozzle leaks in station no. 2 contributed 32.9% and 66.6% to the annual methane emissions, respectively. Leaks from the nozzles connected to the vehicles' onboard tanks were a significant source of emissions due to the long time-fill processes.

The PTT methane emissions of each station were calculated as a ratio between the annual methane emissions and the natural gas supplied to the station. The results showed that under the business-as-usual scenario, the PTT methane emissions from stations nos. 1 and 2 were $1.4 \pm 0.8\%$ and $0.7 \pm 0.7\%$, respectively.

Under the minimal-emission scenario, the PTT methane emissions from station no. 1 could reduce to $0.3 \pm 0.2\%$. In this scenario, the compressors were prevented from starting intermittently

outside the scheduled refueling hours and the throughput of the station was increased to refueling the maximum number of vehicles possible. Leaks from the station components were eliminated, and twin-hose assemblies were employed to minimize the amount of methane released to the atmosphere from nozzle venting events. The PTT methane emissions from station no. 2 could potentially reduce to 0.013 ± 0.003% if compressor emissions were kept at a minimum, and component and nozzle leaks were eliminated.

These recommendations, some of which have been implemented, prove that more than 80% of methane emissions from the studied natural gas refueling infrastructure can be eliminated by using available technologies and deploying the best practices to operate these facilities.

5.2 Recommendations for Future Work

The specific objectives of this thesis work were accomplished by deploying the HVS system to perform point-source measurements at two time-fill CNG refueling stations. However, there remain limitations in the present study that should be addressed in future work. The recommendations below would require collaborative efforts between researchers and the operators of the natural gas refueling stations.

First, component-level methane emissions for the compressors in this study were measured for limited time periods. Consequently, emission fluctuations that occurred due to temporal events such as compressor blowdowns were not reflected in the results. Additionally, emission variations caused by the dynamics of two compressors operating in parallel were not captured. Measurements for extended periods of time would increase confidence level in the component-level emission data.

Second, the effectiveness of implementing best practices to reduce methane emissions would ideally be quantified in future work. In the case of station no. 2 presented in this study, emissions from compressor no. 1 after the open drain valve was closed could be quantified. Nozzle venting emissions from station no. 1 could also be measured after the twin-hose assemblies are used.

Third, measurement campaigns at more facilities are generally required to develop comprehensive emission factors for sources within natural gas refueling stations. Selection of sample stations covering a wide range of station ages and technologies, as well as natural gas fuel throughputs, should be carried out in future work.

Finally, applications of the HVS system could be explored to assess the PTT methane emissions from LNG refueling stations and bunkering facilities for heavy-duty vehicles and marine vessels, respectively. To the best of our knowledge, the PTT methane emissions from LNG refueling stations reported by Clark et al. [19] represent the only published data in the scientific literature. Clark et al. estimated methane emissions from the LNG offloading process by assuming that the LNG remained in the transfer line has to be released to the atmosphere at the end of an offloading process. Direct quantification was not conducted due to access restrictions which resulted in a high uncertainty in emission measurements from LNG offloading processes. In addition, methane emissions from each of the stages in the LNG offloading processes including precooling, purging, filling, and inerting were not characterized.

References

[1] J. Rogelj, M. Den Elzen, N. Höhne, T. Fransen, H. Fekete, H. Winkler, R. Schaeffer, F. Sha, K. Riahi, M. Meinshausen, Paris Agreement climate proposals need a boost to keep warming well below 2 °C, Nature. 534 (2016) 631–639. doi:10.1038/nature18307.

[2] J.L. Osorio-Tejada, E. Llera-Sastresa, S. Scarpellini, Liquefied natural gas: Could it be a reliable option for road freight transport in the EU?, Renew. Sustain. Energy Rev. 71 (2017) 785–795. doi:10.1016/j.rser.2016.12.104.

[3] Natural Resources Canada, Energy Fact Book 2019-2020, 2019. https://www.nrcan.gc.ca/science-data/data-analysis/energy-data-analysis/energy-facts/20061.

[4] Environment and Climate Change Canada, National Inventory Report 1990-2017: Greenhouse Gas Sources and Sinks in Canada: Part 3, Gatineau, 2019. https://www.canada.ca/en/environment-climate-change/services/climate-change/greenhouse-gas-emissions/inventory.html.

[5] A. Thiruvengadam, M. Besch, V. Padmanaban, S. Pradhan, B. Demirgok, Natural gas vehicles in heavy-duty transportation-A review, Energy Policy. 122 (2018) 253–259. doi:10.1016/j.enpol.2018.07.052.

[6] A. García-Olivares, J. Solé, O. Osychenko, Transportation in a 100% renewable energy system, Energy Convers. Manag. 158 (2018) 266–285. doi:10.1016/j.enconman.2017.12.053.

[7] J. Speirs, P. Balcombe, P. Blomerus, M. Stettler, P. Achurra-Gonzalez, M. Woo, D. Ainalis, J. Cooper, A. Sharafian, W. Mérida, D. Crow, S. Giarola, N. Shah, N. Brandon, A. Hawkes,

Natural gas fuel and greenhouse gas emissions in trucks and ships, Prog. Energy. (2019) 0–18. https://doi.org/10.1088/2516-1083/ab56af.

[8] H. Cai, A. Burnham, R. Chen, M. Wang, Wells to wheels: Environmental implications of natural gas as a transportation fuel, Energy Policy. 109 (2017) 565–578. doi:10.1016/j.enpol.2017.07.041.

[9] D.C. Quiros, A. Thiruvengadam, S. Pradhan, M. Besch, P. Thiruvengadam, B. Demirgok, D. Carder, A. Oshinuga, T. Huai, S. Hu, Real-world emissions from modern heavy-duty diesel, natural gas, and hybrid diesel trucks operating along major california freight corridors, Emiss. Control Sci. Technol. 2 (2016) 156–172. doi:10.1007/s40825-016-0044-0.

[10] A. Thiruvengadam, M.C. Besch, P. Thiruvengadam, S. Pradhan, D. Carder, H. Kappanna, M. Gautam, A. Oshinuga, H. Hogo, M. Miyasato, Emission rates of regulated pollutants from current technology heavy-duty diesel and natural gas goods movement vehicles, Environ. Sci. Technol. 49 (2015) 5236–5244. doi:10.1021/acs.est.5b00943.

[11] F. Tong, P. Jaramillo, I.M.L. Azevedo, Comparison of life cycle greenhouse gases from natural gas pathways for medium and heavy-duty vehicles, Environ. Sci. Technol. 49 (2015) 7123–7133. doi:10.1021/es5052759.

[12] S.P.A. Brown, Natural gas vs. oil in U.S. transportation: Will prices confer an advantage to natural gas?, Energy Policy. 110 (2017) 210–221. doi:10.1016/j.enpol.2017.08.018.

[13] Natural Resources Canada, Natural Gas Facts, (2019). https://www.nrcan.gc.ca/science-data/data-analysis/energy-data-analysis/energy-facts/natural-gas-facts/20067 (accessed December 18, 2019).

[14] Y. Fan, A. Lee, N. Parker, D. Scheitrum, A.M. Jaffe, R. Dominguez-Faus, K. Medlock,

Geospatial, temporal and economic analysis of alternative fuel infrastructure: The case of freight and U.S. Natural Gas Markets, Energy J. 38 (2017) 199–230. doi:10.5547/01956574.38.6.yfan.

[15] J. Ogden, A.M. Jaffe, D. Scheitrum, Z. McDonald, M. Miller, Natural gas as a bridge to hydrogen transportation fuel: Insights from the literature, Energy Policy. 115 (2018) 317–329. doi:10.1016/j.enpol.2017.12.049.

[16] N.N. Clark, D.R. Johnson, D.L. McKain, W.S. Wayne, H. Li, J. Rudek, R.A. Mongold, C. Sandoval, A.N. Covington, J.T. Hailer, Future methane emissions from the heavy-duty natural gas transportation sector for stasis, high, medium, and low scenarios in 2035, J. Air Waste Manag. Assoc. 67 (2017) 1328–1341. doi:10.1080/10962247.2017.1368737.

[17] J.R. Camuzeaux, R.A. Alvarez, S.A. Brooks, J.B. Browne, T. Sterner, Influence of methane emissions and vehicle efficiency on the climate implications of heavy-duty natural gas trucks, Environ. Sci. Technol. 49 (2015) 6402–6410. doi:10.1021/acs.est.5b00412.

[18] Intergovernmental Panel on Climate Change, Anthropogenic and Natural Radiative Forcing, in: Intergovernmental Panel on Climate Change (Ed.), Clim. Chang. 2013 - Phys. Sci. Basis, Cambridge University Press, Cambridge, 2014: pp. 659–740. doi:10.1017/CBO9781107415324.018.

[19] N.N. Clark, D.L. McKain, D.R. Johnson, W.S. Wayne, H. Li, V. Akkerman, C. Sandoval, A.N. Covington, R.A. Mongold, J.T. Hailer, O.J. Ugarte, Pump-to-wheels methane emissions from the heavy-duty transportation sector, Environ. Sci. Technol. 51 (2017) 968–976. doi:10.1021/acs.est.5b06059.

[20] U.S. Department of Energy, Compressed Natural Gas Fueling Stations, Altern. Fuels Data Cent. (2019). https://afdc.energy.gov/fuels/natural_gas_cng_stations.html (accessed

December 23, 2019).

[21] A. Sharafian, S.R. Asaee, O.E. Herrera, W. Mérida, Policy implications of liquefied natural gas use in heavy-duty vehicles: Examples in Canada and British Columbia, Transp. Res. Part D Transp. Environ. 69 (2019) 123–140. doi:10.1016/j.trd.2019.01.021.

[22] D.T. Allen, A.P. Pacsi, D.W. Sullivan, D. Zavala-Araiza, M. Harrison, K. Keen, M.P. Fraser, A.D. Hill, R.F. Sawyer, J.H. Seinfeld, Methane emissions from process equipment at natural gas production sites in the United States: Pneumatic controllers, Environ. Sci. Technol. 49 (2015) 633–640. doi:10.1021/es5040156.

[23] D.T. Allen, D.W. Sullivan, D. Zavala-Araiza, A.P. Pacsi, M. Harrison, K. Keen, M.P. Fraser, A.D. Hill, B.K. Lamb, R.F. Sawyer, J.H. Seinfeld, Methane emissions from process equipment at natural gas production sites in the United States: Liquid unloadings, Environ. Sci. Technol. 49 (2015) 641–648. doi:10.1021/es504016r.

[24] H.L. Brantley, E.D. Thoma, W.C. Squier, B.B. Guven, D. Lyon, Assessment of methane emissions from oil and gas production pads using mobile measurements, Environ. Sci. Technol. 48 (2014) 14508–14515. doi:10.1021/es503070q.

[25] A.L. Mitchell, D.S. Tkacik, J.R. Roscioli, S.C. Herndon, T.I. Yacovitch, D.M. Martinez, T.L. Vaughn, L. Williams, M.R. Sullivan, C. Floerchinger, M. Omara, R. Subramanian, D. Zimmerle, A.J. Marchese, A.L. Robinson, Measurements of methane emissions from natural gas gathering facilities and processing plants: Measurement results, Environ. Sci. Technol. 49 (2015) 3219–3227. doi:DOI: 10.1021/es5052809.

[26] J.R. Roscioli, T.I. Yacovitch, C. Floerchinger, A.L. Mitchell, D.S. Tkacik, R. Subramanian, D.M. Martinez, T.L. Vaughn, L. Williams, D. Zimmerle, A.L. Robinson, S.C. Herndon, A.J. Marchese, Measurements of methane emissions from natural gas gathering facilities

and processing plants: Measurement methods, Atmos. Meas. Tech. 8 (2015) 2017–2035. doi:10.5194/amt-8-2017-2015.

[27] A.J. Marchese, T.L. Vaughn, D.J. Zimmerle, D.M. Martinez, L.L. Williams, A.L. Robinson, A.L. Mitchell, R. Subramanian, D.S. Tkacik, J.R. Roscioli, S.C. Herndon, Methane emissions from United States natural gas gathering and processing, Environ. Sci. Technol. 49 (2015) 10718–10727. doi:10.1021/acs.est.5b02275.

[28] R. Subramanian, L.L. Williams, T.L. Vaughn, D. Zimmerle, J.R. Roscioli, S.C. Herndon, T.I. Yacovitch, C. Floerchinger, D.S. Tkacik, A.L. Mitchell, M.R. Sullivan, T.R. Dallmann, A.L. Robinson, Methane emissions from natural gas compressor stations in the transmission and storage sector: Measurements and comparisons with the EPA greenhouse gas reporting program protocol, Environ. Sci. Technol. 49 (2015) 3252–3261. doi:10.1021/es5060258.

[29] D.J. Zimmerle, L.L. Williams, T.L. Vaughn, C. Quinn, R. Subramanian, G.P. Duggan, B. Willson, J.D. Opsomer, A.J. Marchese, D.M. Martinez, A.L. Robinson, Methane emissions from the natural gas transmission and storage system in the United States, Environ. Sci. Technol. 49 (2015) 9374–9383. doi:10.1021/acs.est.5b01669.

[30] B.K. Lamb, S.L. Edburg, T.W. Ferrara, T. Howard, M.R. Harrison, C.E. Kolb, A. Townsend-Small, W. Dyck, A. Possolo, J.R. Whetstone, Direct measurements show decreasing methane emissions from natural gas local distribution systems in the United States, Environ. Sci. Technol. 49 (2015) 5161–5169. doi:10.1021/es505116p.

[31] K. McKain, A. Down, S.M. Raciti, J. Budney, L.R. Hutyra, C. Floerchinger, S.C. Herndon, T. Nehrkorn, M.S. Zahniser, R.B. Jackson, N. Phillips, S.C. Wofsy, Methane emissions from natural gas infrastructure and use in the urban region of Boston, Massachusetts, Proc. Natl. Acad. Sci. 112 (2015) 1941–1946. doi:10.1073/pnas.1416261112.

[32] B.K. Lamb, M.O.L. Cambaliza, K.J. Davis, S.L. Edburg, T.W. Ferrara, C. Floerchinger, A.M.F. Heimburger, S. Herndon, T. Lauvaux, T. Lavoie, D.R. Lyon, N. Miles, K.R. Prasad, S. Richardson, J.R. Roscioli, O.E. Salmon, P.B. Shepson, B.H. Stirm, J. Whetstone, Direct and indirect measurements and modeling of methane emissions in Indianapolis, Indiana, Environ. Sci. Technol. 50 (2016) 8910–8917. doi:10.1021/acs.est.6b01198.

[33] J.C. Von Fischer, D. Cooley, S. Chamberlain, A. Gaylord, C.J. Griebenow, S.P. Hamburg, J. Salo, R. Schumacher, D. Theobald, J. Ham, Rapid, vehicle-based identification of location and magnitude of urban natural gas pipeline leaks, Environ. Sci. Technol. 51 (2017) 4091–4099. doi:10.1021/acs.est.6b06095.

[34] National Academies of Sciences Engineering and Medicine, Improving Characterization of Anthropogenic Methane Emissions in the United States, Washington DC, 2018. doi:10.17226/24987.

[35] T.A. Fox, T.E. Barchyn, D. Risk, A.P. Ravikumar, C.H. Hugenholtz, A review of close-range and screening technologies for mitigating fugitive methane emissions in upstream oil and gas, Environ. Res. Lett. 14 (2019). doi:10.1088/1748-9326/ab20f1.

[36] J. Mønster, P. Kjeldsen, C. Scheutz, Methodologies for measuring fugitive methane emissions from landfills – A review, Waste Manag. 87 (2019) 835–859. doi:10.1016/j.wasman.2018.12.047.

[37] T.N. Lavoie, P.B. Shepson, M.O.L. Cambaliza, B.H. Stirm, A. Karion, C. Sweeney, T.I. Yacovitch, S.C. Herndon, X. Lan, D. Lyon, Aircraft-based measurements of point source methane emissions in the Barnett Shale Basin, Environ. Sci. Technol. 49 (2015) 7904–7913. doi:10.1021/acs.est.5b00410.

[38] B.J. Nathan, L.M. Golston, A.S. O'Brien, K. Ross, W.A. Harrison, L. Tao, D.J. Lary, D.R.

Johnson, A.N. Covington, N.N. Clark, M.A. Zondlo, Near-field characterization of methane emission variability from a compressor station using a model aircraft, Environ. Sci. Technol. 49 (2015) 7896–7903. doi:10.1021/acs.est.5b00705.

[39] T.L. Vaughn, C.S. Bell, T.I. Yacovitch, J.R. Roscioli, S.C. Herndon, S. Conley, S. Schwietzke, G.A. Heath, G. Pétron, D. Zimmerle, Comparing facility-level methane emission rate estimates at natural gas gathering and boosting stations, Elem Sci Anth. 5 (2017) 71. doi:10.1525/elementa.257.

[40] A. Gvakharia, E.A. Kort, A. Brandt, J. Peischl, T.B. Ryerson, J.P. Schwarz, M.L. Smith, C. Sweeney, Methane, black carbon, and ethane emissions from natural gas flares in the Bakken Shale, North Dakota, Environ. Sci. Technol. 51 (2017) 5317–5325. doi:10.1021/acs.est.6b05183.

[41] A.M. Fredenslund, J. Hinge, M.A. Holmgren, S.G. Rasmussen, C. Scheutz, On-site and ground-based remote sensing measurements of methane emissions from four biogas plants: A comparison study, Bioresour. Technol. 270 (2018) 88–95. doi:10.1016/j.biortech.2018.08.080.

[42] X. Lan, R. Talbot, P. Laine, A. Torres, Characterizing fugitive methane emissions in the Barnett Shale area using a mobile laboratory, Environ. Sci. Technol. 49 (2015) 8139–8146. doi:10.1021/es5063055.

[43] D.R. Johnson, A.N. Covington, N.N. Clark, Methane emissions from leak and loss audits of natural gas compressor stations and storage facilities, Environ. Sci. Technol. 49 (2015) 8132–8138. doi:10.1007/s10620-017-4599-6.

[44] T.L. Vaughn, C.S. Bell, C.K. Pickering, S. Schwietzke, G.A. Heath, G. Pétron, D.J. Zimmerle, R.C. Schnell, D. Nummedal, Temporal variability largely explains top-

down/bottom-up difference in methane emission estimates from a natural gas production region, Proc. Natl. Acad. Sci. (2018) 201805687. doi:10.1073/pnas.1805687115.

[45] S. Conley, I. Faloona, S. Mehrotra, M. Suard, D.H. Lenschow, C. Sweeney, S. Herndon, S. Schwietzke, G. Pétron, J. Pifer, E.A. Kort, R. Schnell, Application of Gauss's theorem to quantify localized surface emissions from airborne measurements of wind and trace gases, Atmos. Meas. Tech. 10 (2017) 3345–3358. doi:10.5194/amt-10-3345-2017.

[46] D.R. Johnson, A.N. Covington, N.N. Clark, Design and use of a full flow sampling system (FFS) for the quantification of methane emissions, J. Vis. Exp. (2016) 1–14. doi:10.3791/54179.

[47] Climate and Clean Air Coalition, CCAC Oil and Gas Methane Partnership: Methane Emissions Detection and Measurement Techniques, Equipment and Costs, (2015). https://www.epa.gov/sites/production/files/2016-04/documents/mon7ccacemissurvey.pdf (accessed January 7, 2020).

[48] J.I. Connolly, R.A. Robinson, T.D. Gardiner, Assessment of the Bacharach Hi Flow® Sampler characteristics and potential failure modes when measuring methane emissions, Meas. J. Int. Meas. Confed. 145 (2019) 226–233. doi:10.1016/j.measurement.2019.05.055.

[49] T. Howard, T.W. Ferrara, A. Townsend-Small, Sensor transition failure in the high flow sampler: Implications for methane emission inventories of natural gas infrastructure, J. Air Waste Manag. Assoc. 65 (2015) 856–862. doi:10.1080/10962247.2015.1025925.

[50] R.A. Alvarez, D.R. Lyon, A.J. Marchese, A.L. Robinson, S.P. Hamburg, Possible malfunction in widely used methane sampler deserves attention but poses limited implications for supply chain emission estimates, Elem. Sci. Anthr. 4 (2016) 000137. doi:10.12952/journal.elementa.000137.

[51] Bacharach, Hi Flow Sampler, (2015). https://www.mybacharach.com/wp-content/uploads/2015/08/0055-9017-Rev-7.pdf (accessed December 19, 2019).

[52] D. Johnson, R. Heltzel, Methane emissions measurements of natural gas components using a utility terrain vehicle and portable methane quantification system, Atmos. Environ. 144 (2016) 1–7. doi:10.1016/j.atmosenv.2016.08.065.

[53] D. Johnson, R. Heltzel, D. Oliver, Temporal variations in methane emissions from an unconventional well site, ACS Omega. 4 (2019) 3708–3715. doi:10.1021/acsomega.8b03246.

[54] D. Johnson, A. Covington, N. Clark, Environmental and economic assessment of leak and loss audits at natural gas compressor and storage facilities, Energy Technol. 2 (2014) 1027–1032. doi:10.1002/ente.201402086.

[55] Los Gatos Research, Ultraportable Greenhouse Gas Analyzer (CH4, CO2, H2O), (2019). http://www.lgrinc.com/analyzers/ultraportable-greenhouse-gas-analyzer/ (accessed December 19, 2019).

[56] Bascom-Turner Instruments, Gas-Explorer Detectors Operation Manual, (2008). https://www.bascomturner.com/gas-explorer.php (accessed January 7, 2020).

[57] J.R. Taylor, Introduction to Error Analysis, University Science Books, Sausalito, 1997.

[58] D.S. Baer, J.B. Paul, M. Gupta, A. O'Keefe, Sensitive absorption measurements in the near-infrared region using off-axis integrated-cavity-output spectroscopy, Appl. Phys. B Lasers Opt. 75 (2002) 261–265. doi:10.1007/s00340-002-0971-z.

[59] Y.A. Çengel, M.A. Boles, Thermodynamics: An Engineering Approach, 8th ed., McGraw-Hill Education, Boston, 2015.

Appendices

Appendix A Greenhouse Gas Analyzer

A.1 Off-Axis Integrated Cavity Output Spectroscopy

A schematic diagram of the GHG analyzer based on the off-axis ICOS technology is shown in Figure 26. The gas sample flows through a cylindrical tubular measuring cell sealed by high-reflectivity mirrors on its ends. The temperature and pressure of the gas sample inside the cell are measured. A diode laser beam is directed through the gas sample and makes thousands of passes to create an effective optical path length of several thousand meters before leaving the cell into a photodetector. A solid etalon is used to measure the relative wavelength of the laser, which is tuned over the absorption features of the target species (e.g., methane). The mole fractions of methane, carbon dioxide, and water vapor are determined from the measured absorption of the gas sample in the near-infrared region using Beer's Law [55,58].

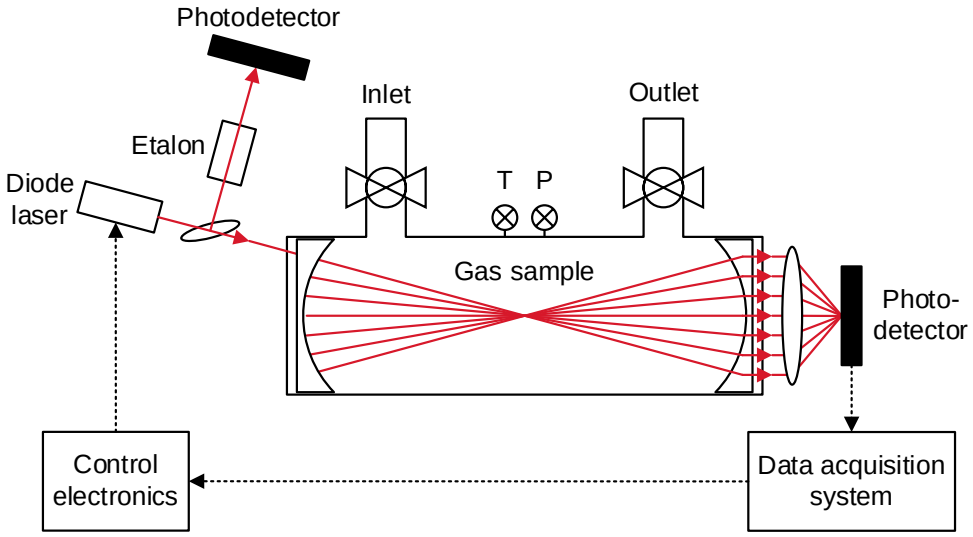

Figure 26. A schematic diagram of the GHG analyzer based on the off-axis ICOS technology.

A.2 Greenhouse Gas Analyzer Referencing

The GHG analyzer was referenced against secondary methane concentration standards of 3,990 ± 40 ppm, 1.004 ± 0.020%, and 4.016 ± 0.080%. The results of the referencing are presented in Figure 27. The maximum discrepancy between the methane standard gas concentrations and the measured values by the GHG analyzer was 1.6%.

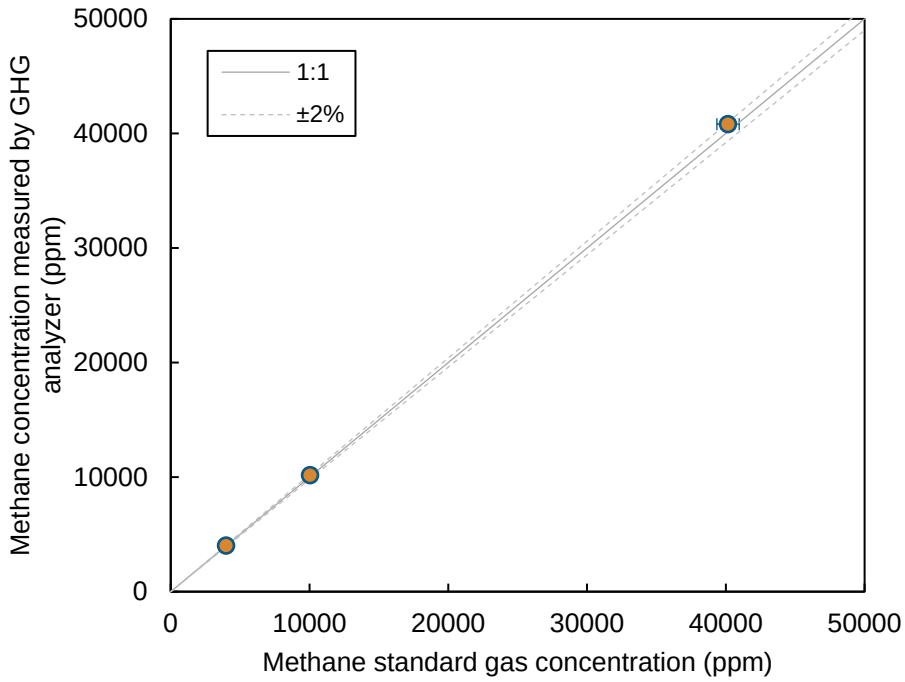

Figure 27. GHG analyzer referencing results against standard gases with methane concentrations of 3,990 ± 40 ppm, 1.004 ± 0.020%, and 4.016 ± 0.080%.

Appendix B Derivation of High-Volume Sampling Formula

The derivation of the methane mass flow rate shown in Eq. (1) is as follows. $\dot{m}_{CH_4}$ is the methane mass flow rate (g/h), $\dot{V}_{CH_4}$ is the standard volumetric flow rate of methane (m^3/h), and ρ_{CH_4} is the density of methane at standard condition (g/m^3).

$\dot{V}_m$ is the standard volumetric flow rate of natural gas-air mixture (m^3/h), and C_{CH_4} is the net mole fraction of methane. Using Dalton's and Amagat's laws for ideal gas mixtures [59], the mole fraction of methane in a natural-gas air mixture is equal to the partial pressure or volume of methane (i.e., $C_{CH_4} = \frac{P_{CH_4}}{P_m} = \frac{V_{CH_4}}{V_m}$). Hence, $\dot{V}_{CH_4} = \dot{V}_m\, C_{CH_4}$. $C_{CH_4,out}$ and $C_{CH_4,in}$ are the exhaust and background methane mole fractions. Eq. (A.2.1) gives the methane mass flow rate as a function of exhaust and background methane mole fractions:

$$\begin{aligned} \dot{m}_{CH_4} &= \dot{V}_{CH_4}\, \rho_{CH_4} \\ &= \dot{V}_m\, C_{CH_4}\, \rho_{CH_4} \\ &= \dot{V}_m \left(C_{CH_4,out} - C_{CH_4,in}\right) \rho_{CH_4} \end{aligned} \tag{A.2.1}$$

As the expected methane concentration in the flow passing through the HVS system is less than 5% (50,000 ppm), it is assumed that the standard volumetric flow rate of the natural gas-air mixture is equal to the standard volumetric flow rate of air, $\dot{V}_{air}$. Therefore, Eq. (A.2.1) can be simplified:

$$\dot{m}_{CH_4} = \dot{V}_{air}\, \rho_{CH_4} \left(C_{CH_4,out} - C_{CH_4,in}\right) \times 10^{-6} \tag{A.2.2}$$

where, the exhaust and background methane mole fractions are expressed in the unit of parts per million (ppm).